MSC Adams modelling of mechanical system in A400M Crew Entrance Door

David Lindberg

Division of Mechanics

Abstract

This report is an official version of the master thesis report, where some pictures have been removed for Intellectual Property reasons.

Saab Aerostructures has developed the Crew Entrance Door (CED) for Airbus A400M. Airbus has decided some different load cases for which the Crew Entrance Door must be built to withstand without something breaking down.

The door is maneuvered by a mechanical system and the load cases are essential for the sizing of the components in the mechanical system. Saab has previously used MS Excel to analytically calculate resulting forces in the mechanical system due to external and/or internal loads in the different load cases. This report describes how the mechanical system for A400M Crew Entrance Door instead can be modeled and solved numerically with the computer program MSC Adams/View.

Creating a model of a mechanical system in MSC Adams/View proved to be easy and fairly quick. The benefit of working with MSC Adams instead of MS Excel is that it is quicker and more user friendly.

The major differences when comparing results were believed to be an effect of comparing results from a kinematic model with results from a dynamic model. Therefore it is in the Authors opinion that the analytical method to calculate resulting forces with MS Excel can be replaced by numerical calculations with MSC Adams/View. However, apart from calculating reaction forces there are additional post-simulation calculations for which it is perhaps more beneficial to use MS Excel. To do these post-simulation calculations in MS Excel it is easy to use exported results from MSC Adams.

If Saab Aerostructures decide to start working with MSC Adams/View and if Saab wants geometry to be imported to the model, then an advise from the Author is to have a software installed which can convert step-files (*.stp or *.step) to the MSC Adams preferred file format Parasolid (*.xmt_txt or *.x_t). The software should also be able to repair geometry which will greatly increase mass accuracy.

Preface

I especially want to thank *Sven-Gunnar Eriksson*, *Bengt Lundqvist* and *Anna Carlsson* at Saab Aerostructures for helping me understand the mechanical system for A400M Crew Entrance Door. I am also greatly thankful to my other colleagues at Saab Aerostructures for helping me with various problems that arose during this work.

I am thankful to my supervisor *Peter Schmidt* and my examiner *Anders Klarbring* at Linköping University for helping me structure my work.

I am also thankful to *Magnus Bergelin* and *Per Hedlund* at Saab for helping me converting files and to *Per Persson* at Saab for helping me learn how MSC Adams/View works.

I would also like to say thanks to my wife *Annika*, for her love and care.

Dokumentslag *Type of document*
REPORT-MSc. Thesis

Reg-nr *Reg. No*
AIF288-2-RE-0496

Infoklass *Info. class*
Öppen

Utgåva *Issue*
A

Sida *Page*
3 (56)

Table of Content

Dokumentslag *Type of document*

REPORT-MSc. Thesis

Infoklass *Info. class*

Öppen

Reg-nr *Reg. No*

AIF288-2-RE-0496

Utgåva *Issue*

A

Sida *Page*

4 (56)

1 INTRODUCTION

1.1 Background

Saab has developed the Crew Entrance Door (CED) for Airbus A400M, a military transport aircraft. The door is maneuvered by a mechanical system for opening/closing and locking/unlocking. In addition the mechanical system can, in case of emergency evacuation in flight, release the door from the aircraft (jettison).

Airbus has decided some different load cases which the CED must be able to withstand without something breaking down in the mechanical system. Saab has previously used MS Excel to analytically calculate resulting forces in the mechanical system due to external and/or internal loads in the different load cases. The approach led to large and complex MS Excel sheets. This report describes how the mechanical system for A400M Crew Entrance Door instead can be modeled and solved numerically with the computer program MSC Adams/View. The previous calculations using MS Excel are called analytical in this report and the MSC Adams calculations are named numerical.

1.2 Purpose

The purpose with creating an MSC Adams model of the mechanical system for A400M Crew Entrance Door is to see if this program can calculate resulting forces in an easier and more comprehensive way than what is the case when working analytically with MS Excel.

1.3 Limitations

All details on the door have not been modelled. Only the parts included in the mechanical system and a few additional items such as door blade and doorway has been modelled. The mass for the parts on the CED not belonging to the mechanical system have all been added to a common mass applied on the door blade.

In reality some additional steps called foldable steps are included in the mechanical system, however due to project time limitations these have not been modelled.

When jettisoning the door, it will be released from the aircraft after the hinges have rotated more than during normal manoeuvring. The door is released through a mechanism that is forcing apart a connection at the hinge line. In the model this mechanism was simplified to just releasing the door at a certain rotation of the hinges.

1.3.1 Assumptions

The mechanical system was modelled with rigid bodies and joints. Consequently, an assumption has been made that the deformation of the bodies can be neglected.

Friction has been modelled for the contact between rubber sealing and door blade. On the lower side of the door the displacement was assumed to be perpendicular to the surface of the rubber sealing (i.e. no shear displacement) and therefore was friction in that region neglected.

Both of the two assumptions for rigid bodies and friction were also made in the previous analytical method.

1.4 Airbus A400M

Figure 1. Airbus A400M with the Crew Entrance Door pointed out. Picture copied from Airbus Military [1]
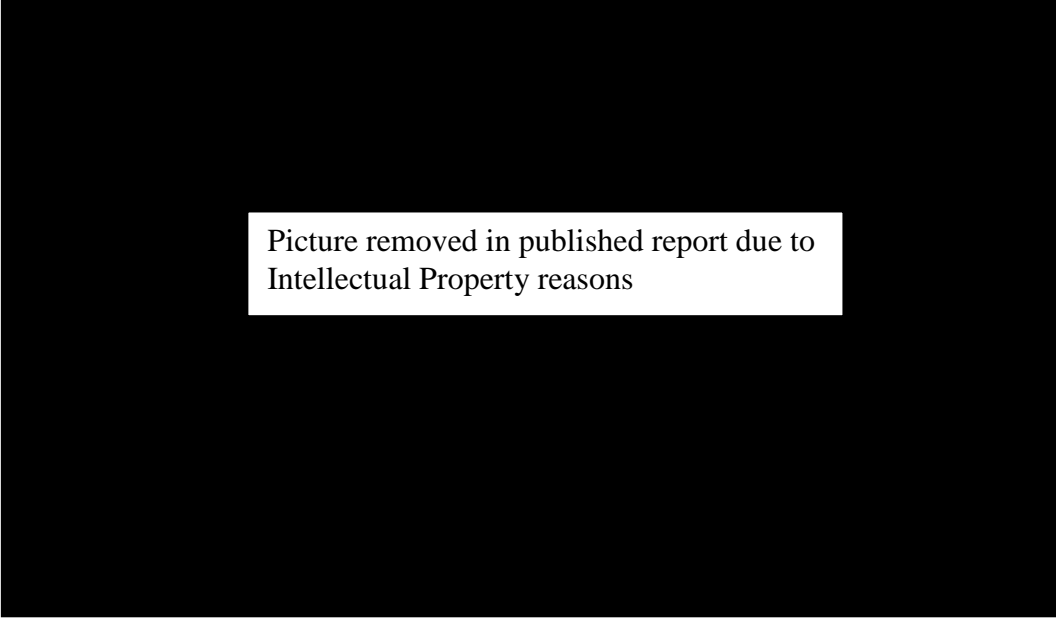
The A400M is a military air transporter with the purpose to replace the ageing fleets of C-130 Hercules and C-160 Transall. The A400M is 45 metres long and have a wing span of over 42 metres. The aircraft is driven by four counter-rotating turboprop engines and have the capacity to load up to 37 tonnes of cargo. The maiden flight took place on 11th December 2009 and by December 2011 a total of 174 aircrafts had been ordered, [1]. Airbus military estimates that the first aircraft is to be delivered to customer early 2013, [2].

1.4.1 Crew Entrance Door – CED

In this subchapter the Crew Entrance Door will be presented shortly.

Picture removed in published report due to Intellectual Property reasons

Figure 2. Complete CED to the left and the mechanical systems in the door to the right

For the CED there are three positions of the door that distinguish the manoeuvre from closed to opened door. The CED can be closed and locked, lifted (unlocked) or opened.

Starting from closed and locked the CED should first be unlocked by lifting the door with either the inner or outer handle, see Figure 2. These two handles lift the door to a position where it is possible for the door to rotate outwards, called lifted position. The door is open when it has fully rotated out to a position where it also works as a staircase for the crew. A wire is then the only thing keeping the door from rotating more than to opened position, see Figure 3.
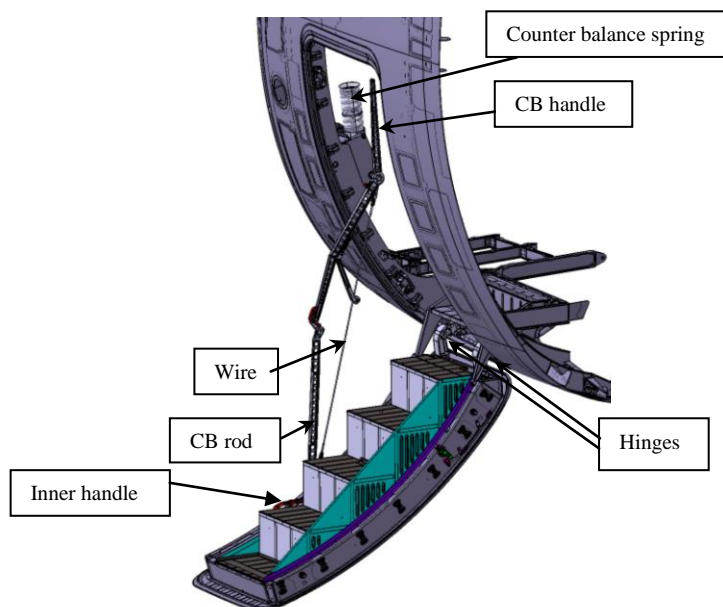
Figure 3. Crew Entrance Door opened

When the door shall be closed the Counter Balance (CB) handle is used, see Figure 2 and Figure 3. The word Counter balance comes from a powerful spring mounted on the CB mechanism that helps the closing manoeuvre by balancing some of the weight of the door, see Figure 2. When the door is closed, with the CB handle, it is still in lifted position and can first then be locked by pulling back either the inner or outer handle.

When operating the jettison handle, see Figure 2, the CB mechanism will be disconnected from the door during the lifting manoeuvre. By disconnecting the CB rod there will be no wire stopping the outward rotation motion of the door and this will cause a larger rotation of the hinges than at normal manoeuvring, which will cause a mechanism to release the door from the fuselage.

The different sides on the CED is not named right or left but instead forward (fwd) or afterward (aft). With forward meaning the direction forward towards the nose of the aircraft, see Figure 4.

Figure 4. Fwd and aft directions for CED. Picture copied from Airbus Military [1]

1.5 Load Cases

Airbus decided some different load cases which the CED must be able to withstand without the door breaking. The different load cases create reaction forces through out the door. Time limitations has made it impossible to compare numerical calculations (MSC Adams) with analytical calculations (MS Excel) for all reaction forces at all locations and therefore only some reaction forces from the different load cases will be presented and compared. The load cases to be compared with analytical (MS Excel) calculations are the following:

1.5.1 Lifting the door

The lifting manoeuvres with either inner, outer or jettison handle were simulated with and without an internal overpressure. The numerically calculated forces that are compared to analytical results are handle loads and reaction forces at Stop1 and Upper Guide, see 3.1.5.1 for more information on Stop1 and Upper Guide.

1.5.2 Jamming during lifting manoeuvre

The lifting manoeuvres were simulated with either the inner or outer handle but with jamming in the mechanical system, at either the gearbox, see Figure 2, or at the outer handle, see Figure 2. A maximum allowed load was applied on the handles and the reaction forces in two rods were calculated. In the result chapter the reaction forces in rod P2P6 and rod P7P10, see Figure 2, are compared with analytical calculations.

1.5.3 Opening the door

The opening manoeuvre was simulated without wind loads but also with wind loads in both closing and opening directions. Reaction forces in hinges and CB rod connection to the door are compared to analytical calculations.

1.5.4 Opened door

In the simulations with the CED in opened position, the external loads were from:
- One man running
- Three men standing
- 60 knots wind load
- Side load on CB arm fwd/aft direction + one man standing on step 1
- Side load on CB handle fwd/aft direction

Numerically calculated reaction forces in hinges, in CB rod and reaction forces in the wire are compared to analytical calculations.

1.5.5 Jettison manoeuvre

The jettison manoeuvre (CED falling outward) was simulated with aerodynamic loads on the door from high speed, low altitude and high angle of attack. Reaction forces at hinges, angular velocity and angular acceleration for the door during jettison are compared with analytical calculations.

2   THEORY - MULTIBODY SYSTEMS

A multibody system, MBS, is a mechanical system of multiple rigid and/or flexible bodies/parts. These bodies (or parts) are joined together for the purpose to transfer motion from one body to another, see Figure 5. This chapter will present why a MBS-program can be a useful tool when trying to build a mechanical system and why results sometimes can be unreliable. Thereafter, it will be shown how a model is built and how the simulations are calculated.
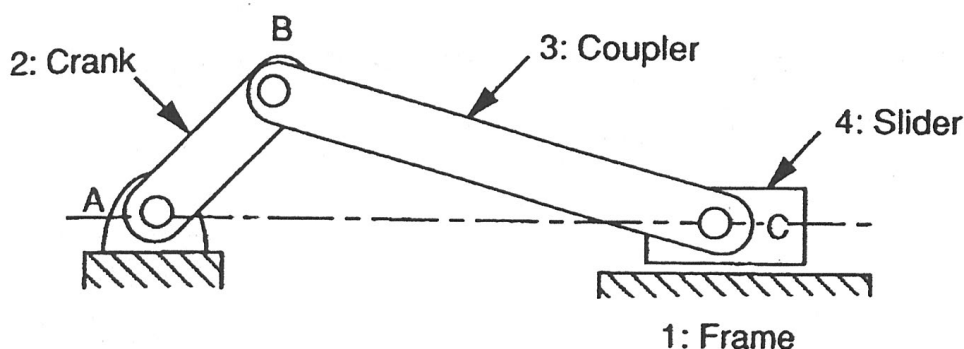

Figure 5. A Slider-Crank mechanism, [3]. The rotation of the crank creates a translational motion for the slider

2.1   Practical use of MBS-programs

MSC Adams is one of many computer programs for modelling and simulating multibody systems, MBS. In MBS-programs a virtual prototype of a mechanism can be built and then simulated. If the results, a certain movement or load transmission are not satisfying, the prototype can easily be modified and then simulated again.

Compared to building real prototypes to undergo testing, this way of work reduce both time and saves money. This is true especially if it takes several adjustments of the prototype to get the desired results, [3].

The virtual prototype of a mechanism in MBS programs is a mathematical model of reality. Since a mathematical model may have different errors due to how it has been built, it is always necessary to build a final real prototype and test it to confirm the results before production is started.

Errors that can occur in MBS models:

- In a model built with rigid bodies the loads in the system are assumed to be so small that it will not introduce neither elastic nor plastic deformation. If the forces applied in the system would in reality give large deformation, the calculated result would differ substantially compared to physical testing, [3].

- A model should not be modelled more complex than necessary for a correct presentation of the system. However if a model is built too simple it may mean that some things that has influence on the motion of the system is not modelled and therefore differs the result compared to physical testing, [3].

- Bad input makes the model a bad approximation of reality. Such inputs could be friction coefficients or stiffness and damping values for springs, [3]. In addition, incorrect geometry may produce big differences in mass and inertia compared to reality.

- A rigid body system should not be modelled with redundant constraints, even if the real mechanical system is such. Redundant constraints can cause high reaction forces that have nothing to do with reality, see 3.1.4.

- When solving differential equations, numerical errors could lead to a solution greatly different from the real solution, [3].

2.2 Build a model

In this subchapter it is described how a model is built by joining parts.

In a mechanical system parts can be connected with something called joints. These joints determine how one part is allowed to move relative to another part. Every joints function is to decrease the mobility for a set of parts and this is done by locking so called *degrees of freedom*, DOF.

A part has initially 6 DOF, three axis directions or any combined direction to translate in and also rotation around those three axes or any combined direction. When parts are joined together, some of the DOF's are locked.

Joints can be divided into two groups; lower and higher pairs. A lower pair is a joint with an area contact between the two bodies. A higher pair is instead a joint with only a point or a line contact, [3].

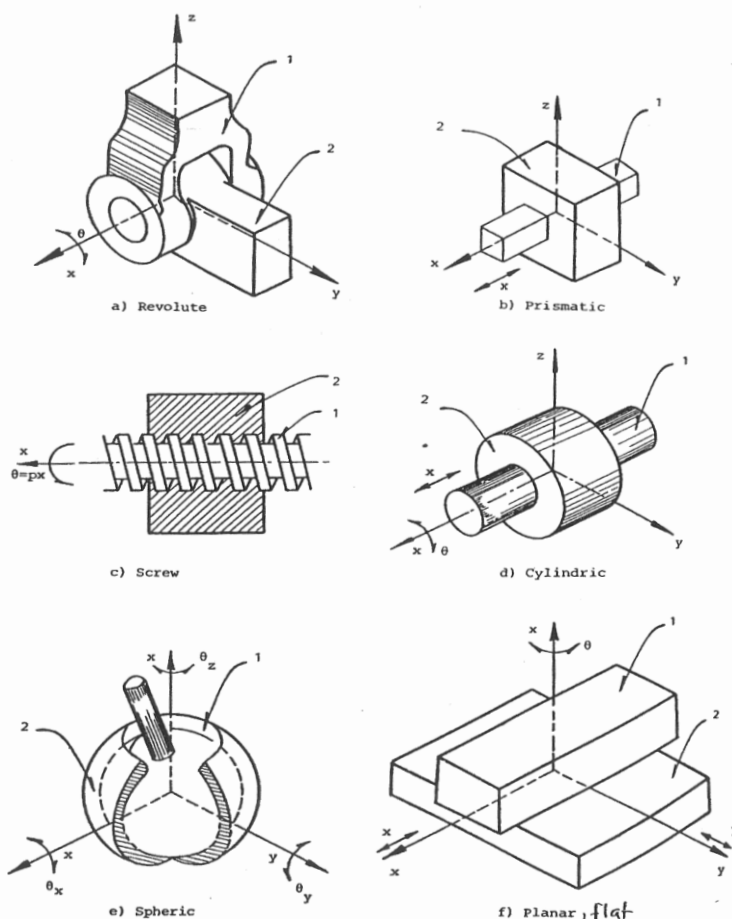|	Dokumentslag *Type of document*	Reg-nr *Reg. No*
SAAB	**REPORT-**MSc. Thesis	AIF288-2-RE-0496
	Infoklass *Info. class*	Utgåva *Issue* Sida *Page*
	Öppen	A 12 (56)

2.2.1 Lower pairs

Figure 6. Kinematic constraints also known as joints, [3]

A spherical joint, see Figure 6e, works very much like a human shoulder as it locks all translations between the two parts (arm and torso) but not the rotations, so there are 3 degrees of freedom left. However, two parts joined together by a spherical joint can also translate and rotate together. This means that a system consisting of two spherical jointed parts have three DOF for their internal rotation, three DOF for their common translation and three DOF for their common rotations adding up to a total of 9 DOF.

A revolute joint, see Figure 6a, works similar to a human knee and precisely as in a knee no translations are allowed between the femur bone and the tibia bone, instead only rotation around one axis is allowed, 1 DOF. In a system consisting of two parts connected with a revolute joint there are 1 DOF for the internal rotation and 6 DOF for the common rotation and translation, adding up to a total of 7 DOF.

A cylindrical joint, see Figure 6d, is similar to a revolute joint but with the difference that a cylindrical joint also allows translation in direction of the rotational axis. Consequently 1 DOF is released between two bodies connected with a cylindrical joint compared to two bodies connected with a revolute joint.

A translational/prismatic joint, see Figure 6b, only allows translation in one direction and allows no rotations at all. A planar joint, see Figure 6f, restrict the two parts so that they must always lie in the same plane. A planar joint can be described as the limitations for a computer mouse to the mouse pad. The computer mouse can be rotated around an axis normal to the desktop and it can also be moved forward/backward and to the sides but are not allowed to lift from the mouse pad.

The sixth joint is the screw joint, see Figure 6c, it works like a cylindrical joint but with the rotation as a function of translation and has therefore one less degree of freedom.

Finally there is an additional joint called a fix joint which locks all 6 degrees of freedom between two bodies.

2.2.2 Higher pairs

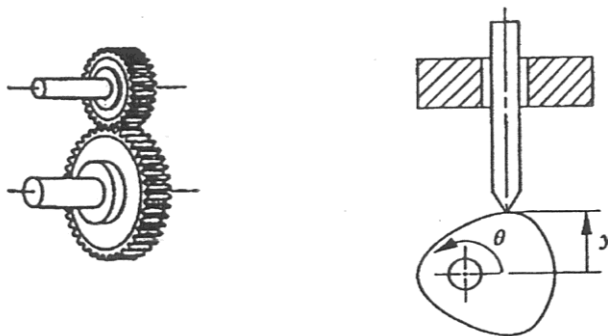In addition to the lower pairs there are a few more joints called higher pairs.

Figure 7. A gear and a cam are two examples of a higher pair, [3]

Gears and cams are examples of higher pairs and in both joints there is always a point contact between the two bodies.

When applying a gear joint, the point and direction for equal velocity must be decided. This point is the point of contact for the gear teeth and from this the gear ratio is calculated. Essential for a gear joint is also that the two bodies must be connected to a common third body, [4].

If there is not a common third body or that the point for equal velocity is unknown, a coupler could be used instead. To apply a coupler between two joints the only thing that has to be input is the ratio.

2.2.3 Driving constraints

If a joint allows rotation or translation then it is possible to apply a motion to that joint. This motion is called a driving constraint and it can be a function of an independent parameter, for example time. When applying a motion the DOF corresponding to that motion are locked.

2.2.4 Forces

In addition to joints and motions also forces can be applied between parts. A force can be constant or a function of an independent parameter (such as time) and it can also for example be programmed so it will act as a spring with or without damping between two parts.

2.2.5 The Contact Function

Bodies in MSC Adams do not by default notice a collision during simulation. One body will move into another as if there were made out of thin air. If it is desired to simulate a collision, then a *Contact* function could be applied on the specific parts.

The Contact has two built-in functions, Impact and Restitution. Simplified, an Impact function works like when two solids occupy the same space then a dampened spring is introduced to try separating the solids. To be more detailed, MSC Adams first calculates the centre of mass for the intersection volume. Then from the centre of mass the closest points on each body's surface are calculated, see Figure 8. The direction of the contact forces is the line between these two points.
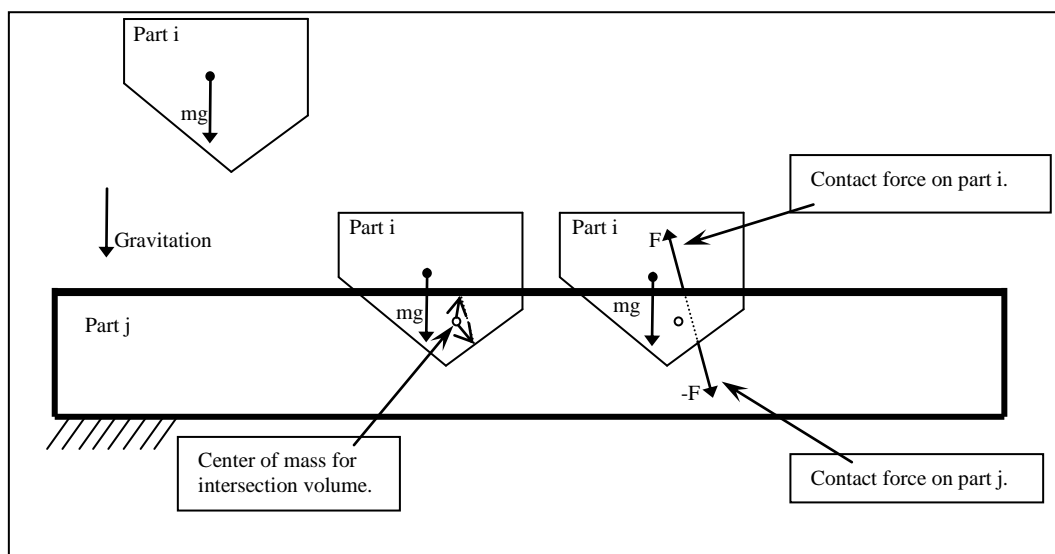

Figure 8. Sketch of how a Contact with Impact function works

The forces in the contact are modelled as if there were springs with adjustable stiffness and maximum damping. At what depth the ramped damping shall act as maximum damping can be decided aswell. The damping is ramped to create a smoother contact. In addition the spring force can also be modified by adjusting a force exponent, *e*, [4].

$$F = kx^e$$

Where *F* is the force, *k* is the stiffness, *x* is the penetration depth and *e* is the force exponent.

The other function in a Contact is the Restitution function. When contact occurs, modelled with the Restitution function, a constant penalty force is applied in the direction opposite the motion. In addition a coefficient of restitution determines the energy loss during the contact. A coefficient of value 1 means that the collision is entirely elastic i.e. no energy losses. However a coefficient of value 0 means that the collision is entirely plastic and there will be no bouncing. MSC Adams has tables with default values for contacts between some different materials in their help manual, [4].

In general, the Impact method is faster and more numerically smooth than the Restitution method. The Impact method also provides a better control of how the contact works, with adjustable distance to maximal damping and force exponent. The Restitution method is the choice to make if the impact parameters are unknown and the coefficient of restitution data is available either from material references or physical testing, [4].

2.3 Simulation

In this chapter the calculations for simulating a mechanical systems is described.

When the MBS-program simulates a model, the computer calculates position, velocity and acceleration for all parts at a given time and also calculates how loads are transferred from one part to another. The user decides how long the simulation shall continue and the size of the time steps to go forward with.

Mechanics can be divided into kinematics and dynamics. In MSC Adams and other MBS programs, a model can be simulated with either a kinematic or a dynamic solver. In the two subchapters Kinematic and Dynamic, the calculations to solve multibody systems are presented.

2.3.1 Kinematic

In kinematic models it is the position, orientation and motion of parts that is of interest. The driving constraints are known and from these, the position and orientation of all bodies are known. A kinematic model is built with zero degrees of freedom therefore do forces not influence the motion in kinematic models, [4]. This means that it is not possible to simulate for example how fast gravity makes a part fall in a kinematic model. However internal forces necessary to hold constraints due to external forces are still calculated.

All equations in this chapter are referred to an unpublished course material for University of Linkoping written by Christensen, Peter [3] unless otherwise explicitly stated.

Let **q** be a matrix containing positions for all parts in the system, i.e. x, y and z coordinates and the angle of rotation around those axes. $\mathbf{H}^k(\mathbf{q})$ is a matrix consisting of all kinematic constraints due to the joints connecting parts, for example a revolute joint.

$$\mathbf{q} = [x_1, y_1, z_1, \theta_1, \phi_1, \varphi_1, \ldots, x_{nb}, y_{nb}, z_{nb}, \theta_{nb}, \phi_{nb}, \varphi_{nb}]^T$$

$$\mathbf{H}^k(\mathbf{q}) = \left[\mathbf{H}^k{}_1(\mathbf{q}), \mathbf{H}^k{}_2(\mathbf{q}), \mathbf{H}^k{}_3(\mathbf{q}), \ldots, \mathbf{H}^k{}_{nk}(\mathbf{q}) \right]^T = \mathbf{0}$$

In a multibody system it is possible to apply a motion to a joint, a driving constraint $\mathbf{H}^d(\mathbf{q},t)$. $\mathbf{H}^d$ can aside from position also be a function of time, [3].

$$\mathbf{H}^d(\mathbf{q},t) = \left[\mathbf{H}^d{}_1(\mathbf{q},t), \mathbf{H}^d{}_2(\mathbf{q},t), \mathbf{H}^d{}_3(\mathbf{q},t), \ldots, \mathbf{H}^d{}_{nk}(\mathbf{q},t) \right]^T = \mathbf{0}$$

Together, the kinematic constraints, $\mathbf{H}^k$, and the driving constraints, $\mathbf{H}^d$, creates the matrix **H**.

$$\mathbf{H}(\mathbf{q},t) = \begin{bmatrix} \mathbf{H}^k(\mathbf{q}) \\ \mathbf{H}^d(\mathbf{q},t) \end{bmatrix} = \mathbf{0}$$

This equation should be solved in order to get the positions, **q**. The nonlinear equation can be solved iteratively by Newton's method. Newton's method begins with a guess of the position, $\mathbf{q}^a$, that is implemented in $\mathbf{H}(\mathbf{q},t)= \mathbf{0}.$ Thereafter an iteration is calculated where the equation first is linearised around $\mathbf{q}^a$.

$$\mathbf{H}(\mathbf{q}^a) + \frac{\partial \mathbf{H}(\mathbf{q}^a)}{\partial \mathbf{q}}(\mathbf{q} - \mathbf{q}^a) = \mathbf{0}$$

$$\left[\mathbf{H_q}(\mathbf{q}^a) \right] \mathbf{d} = -\mathbf{H}(\mathbf{q}^a)$$

Where $\mathbf{H}_q$ is the Jacobian of **H**:

$$\mathbf{H}_q = \frac{\partial \mathbf{H}}{\partial \mathbf{q}}$$

A new iteration point, $\mathbf{q} = \mathbf{q}^a + \mathbf{d}$, is calculated by solving out **d**. The new point is then implemented in $\mathbf{H}(\mathbf{q},t)$ and if $|\mathbf{H}(\mathbf{q})|^2$ is 'small enough' calculations are stopped with **q** as a approximate solution. The value of $|\mathbf{H}(\mathbf{q})|^2$ is also called *error value* and can be set manually. If $|\mathbf{H}(\mathbf{q})|^2$ is not 'small enough', a new iteration is calculated around the new point and so forth until $|\mathbf{H}(\mathbf{q})|^2$ is below

the *error value.* Thereafter the procedure is done again for every time step in the simulation.

The size or number of time steps is decided by the user. The appropriate size of the time steps is depending on how much the parts are moving in the system. If the parts have high acceleration and moves rapidly then shorter time steps might be necessary to get a satisfying value of $|\mathbf{H}(\mathbf{q})|^2$. However if the size of the time steps are too small it can also give a long simulation time.

When the positions, $\mathbf{q}$, for a time step has been calculated then the velocity, $\dot{\mathbf{q}}$, for the same time step can be calculated. The velocity is calculated from the velocity constraint equation acquired after a time derivation of $\mathbf{H}$.

$$\dot{\mathbf{H}}(\mathbf{q},t) = \frac{\partial \mathbf{H}}{\partial \mathbf{q}}\dot{\mathbf{q}} + \frac{\partial \mathbf{H}}{\partial t} = \mathbf{0}$$

$$\mathbf{H_q}\dot{\mathbf{q}} = \mathbf{b}$$

$$\text{where } \mathbf{b} = -\mathbf{H}_t = -\frac{\partial \mathbf{H}}{\partial t} \text{ and } \mathbf{H_q} = \frac{\partial \mathbf{H}}{\partial \mathbf{q}}$$

A second time derivation gives the acceleration constraint equation.

$$\ddot{\mathbf{H}}(\mathbf{q},t) = \frac{d}{dt}\left(\frac{\partial \mathbf{H}}{\partial \mathbf{q}}\dot{\mathbf{q}} + \frac{\partial \mathbf{H}}{\partial t} \right) = \mathbf{0}$$

Which gives:

$$\mathbf{H_q\ddot{q} = c}$$

where $\mathbf{c} = -(\mathbf{H_q\dot{q}})_\mathbf{q}\dot{\mathbf{q}} - 2\mathbf{H}_{\mathbf{q}t}\dot{\mathbf{q}} - \mathbf{H}_{tt}$ and $\mathbf{H}_{tt} = \dfrac{\partial^2\mathbf{H}}{\partial t^2}$; $\mathbf{H}_{\mathbf{q}t} = \dfrac{\partial^2\mathbf{H}}{\partial\mathbf{q}\partial t}$

In addition to the kinematic constraint equations there is an equation of motion to take in account. That equation is derived from Euler's laws and can be written as:

$$\mathbf{M\ddot{q}} + \mathbf{H}_\mathbf{q}^T(\mathbf{q})\boldsymbol{\lambda} = \mathbf{Q}^e(\mathbf{q},\dot{\mathbf{q}},t)$$

Where $\mathbf{M}$ is a matrix containing mass for the system, $\ddot{\mathbf{q}}$ is the acceleration for the parts, $\mathbf{Q}$ is external forces, $\mathbf{H}_\mathbf{q}^T$ is the Jacobian of the constraint equation, $\mathbf{H}(\mathbf{q},t)$, and $\boldsymbol{\lambda}$ is a matrix of the forces between the bodies necessary to uphold the friction free constraints.

To summarize, at every time step the position, velocity and acceleration are calculated with the kinematic constraint equations and the result is implemented in the equation of motion where internal forces are calculated.

2.3.2 Dynamic

The difference between kinematic and dynamic models is that dynamics also take into account how forces affect the motion of the system. In addition, a dynamic model can have one or more degrees of freedom.

In dynamic calculations the kinematic constraints must still be valid, $\mathbf{H}(\mathbf{q},t)=\mathbf{0}$. By combining the kinematic constraints and the equation of motion, a system of so called differential algebraic equations (DAE) is created, [3].

$$\begin{cases} \mathbf{M\ddot{q}} + \mathbf{H}_q^T(\mathbf{q})\boldsymbol{\lambda} = \mathbf{Q}^e(\mathbf{q},\dot{\mathbf{q}},t) \\ \qquad\quad \mathbf{H}(\mathbf{q}) = \mathbf{0} \end{cases}$$

There are different methods to solve dynamic simulations and these methods are called integrators. One integrator might work well on one type of problem but not on another type of problem. It is up to the user to try different integrators to find the most appropriate one for the specific problem. The default integrator for dynamic calculations, in MSC Adams, is the Gear Stiff (GSTIFF) integrator, [4].

2.3.2.1 GSTIFF Integrator

The GSTIFF integrator is the default integrator in MSC Adams and it uses a Backwards Differentiation Formula (BDF) to integrate differential algebraic equations (DAE).

	Dokumentslag *Type of document*	Reg-nr *Reg. No*
SAAB	**REPORT-**MSc. Thesis	AIF288-2-RE-0496
	Infoklass *Info. class*	Utgåva *Issue* Sida *Page*
	Öppen	A 19 (56)

To simulate using the GSTIFF integrator a new variable $\mathbf{u} \equiv \dot{\mathbf{q}}$ is introduced, [5].

$$\begin{cases} \dot{\mathbf{q}} - \mathbf{u} = \mathbf{0} \\ \mathbf{M}\dot{\mathbf{u}} + \mathbf{H}_q^T(\mathbf{q})\lambda = \mathbf{Q}^e(\mathbf{q},\mathbf{u},t) \\ \mathbf{H}(\mathbf{q}) = \mathbf{0} \end{cases}$$

If the DAE is to be solved for a time interval $[t_s,t_e]$, then n time steps are created so that $[t_0=t_s,t_1,\ldots,t_n=t_e]$. The Backward Difference Formula uses values from the previous time steps to calculate velocity and acceleration. This is illustrated using a Backward Euler approximation, [3]:

$$\dot{\mathbf{u}}(t_k) = \frac{\mathbf{u}(t_k) - \mathbf{u}(t_{k-1})}{t_k - t_{k-1}} = \frac{\mathbf{u} - \mathbf{u}_{old}}{h}$$

$$\dot{\mathbf{q}}(t_k) = \frac{\mathbf{q}(t_k) - \mathbf{q}(t_{k-1})}{t_k - t_{k-1}} = \frac{\mathbf{q} - \mathbf{q}_{old}}{h}$$

Inserting these approximations into the DAE gives:

$$(*)\begin{cases} \mathbf{M}\left(\dfrac{\mathbf{u} - \mathbf{u}_{old}}{h}\right) + \mathbf{H}_q^T(\mathbf{q})\lambda - \mathbf{Q}^e(\mathbf{q},\mathbf{u},t) = \mathbf{0} \\ \dfrac{\mathbf{q} - \mathbf{q}_{old}}{h} - \mathbf{u} = \mathbf{0} \\ \mathbf{H}(\mathbf{q}) = \mathbf{0} \end{cases}$$

This system shall then be solved for **q,u** and λ.

There exist several other integrators that solve the DAE in more or less similar ways. Those integrators will not be presented in this report.

2.3.2.2 Index Reduction Methods and Formulations

An index of a DAE is equal to the number of time derivatives necessary to convert the DAE to Ordinary Differential Equations, ODE. The lower the index number is, the easier the equations are to solve numerically. Therefore it is often a good idea to try and lower the index number, [5].

For example, equation (*) above is in the default formulation I3 (Index 3). GSTIFF with I3 formulation is often quick to solve but it also have disadvantages. As seen in the matrix below, the Jacobian of the equation (*) becomes singular when step sizes, *h*, heads towards zero. Therefore might small step sizes for the GSTIFF with the I3 formulation, cause great difficulty for the calculations, [5].

$$\mathbf{G}(\mathbf{x}) = \mathbf{0}; \mathbf{x} \equiv \begin{bmatrix} \mathbf{u} \\ \mathbf{q} \\ \lambda \end{bmatrix}$$

$$\frac{\partial \mathbf{G}}{\partial \mathbf{x}} = \begin{bmatrix} \frac{1}{h}\mathbf{M} - \mathbf{Q_u}^e & \mathbf{H_{qq}}^T \lambda - \mathbf{Q_q}^e & \mathbf{H_q}^T \\ -\mathbf{I} & \frac{1}{h}\mathbf{I} & \mathbf{0} \\ \mathbf{0} & \mathbf{H_q} & \mathbf{0} \end{bmatrix}$$

To lower the risk of a singular Jacobian an index reduction method (IRM) can be used. The IRM is based on exchanging some of the equations in the DAE with time derivatives of the same equations. For example, the kinematic constraint equation can be replaced with the time derivative of the same kinematic constraint equation.

$$(**) \begin{cases} \mathbf{M}\left(\dfrac{\mathbf{u}(t_k) - \mathbf{u}(t_{k-1})}{t_k - t_{k-1}} \right) + \mathbf{H}_q^T(\mathbf{q})\lambda - \mathbf{Q}^e(\mathbf{q},\mathbf{u},t) = \mathbf{0} \\ \dfrac{\mathbf{q}(t_k) - \mathbf{q}(t_{k-1})}{t_k - t_{k-1}} - \mathbf{u} = \mathbf{0} \\ \underline{\dot{\mathbf{H}}(\mathbf{q}) = \mathbf{0}} \end{cases}$$

By using equation (**) above instead of equation (*), the Jacobian does not become singular with small step sizes, [5].

However this also means that the original kinematic constraint does not need to be fulfilled. So instead of having a kinematic equation saying that the distance between parts in a joint must be zero now instead an equation is used where the velocity between parts in a joint shall be zero. A complication due to this modification can be that parts in the model might slowly drift away after some simulation time, a so called drift-off, [5].

In MCS Adams there are a few different formulations to choose of when simulating a model. If there is drift-off issues then the default I3 formulation can be replaced by the SI2 (stabilized index 2) formulation.

In SI2, some modifications are introduced:

$$\begin{cases} \mathbf{M}\dot{\mathbf{u}} + \mathbf{H}_q^T(\mathbf{q})\lambda - \mathbf{Q}^e(\mathbf{q},\mathbf{u},t) = \mathbf{0} \\ \mathbf{u} - \dot{\mathbf{q}} + \mathbf{H}_q^T(\mathbf{q}) = \mathbf{0} \\ \dot{\mathbf{H}}(\mathbf{q},\mathbf{u},t) = \mathbf{0} \\ \mathbf{H}(\mathbf{q},t) = \mathbf{0} \end{cases}$$

Using the SI2 formulation, both the velocity and position equations are fulfilled giving a non-singular Jacobian and preventing drift-off.

Running GSTIFF with SI2 is 25%-100% slower than GSTIFF with I3 formulation at the same error value. However the SI2 formulation usually allows a 10 to a 100 times larger error value than I3 to produce result with the same accuracy and can therefore be simulated with larger time steps, [5].

There exist several other formulations for DAE and those will not be presented in this report.

3   METHOD

This chapter with subchapters describes the method in how the MSC Adams model was built.

3.1   Building the model

The numerical model of the CED was built in MSC Adams as a dynamic model with forces affecting the motions of the bodies. However the analytical calculations done in MS Excel were on a kinematic model of the CED. The reason why modelling the CED as a dynamic model, was to easily be able to calculate the velocity and acceleration of rotation for the hinges during jettison. By simulating the other cases with a slow and constant motion of the bodies, the dynamic calculations were assumed to be similar to the kinematic calculations.

3.1.1   Identifying joints

The CED was modelled in closed and locked position. Drawings and reports of the CED were studied to be able to connect parts with the correct joints. The coordinate system in the MSC Adams model was set equal to the coordinate system used in a Catia CAD model of the CED in closed and locked position. This way positions for the joints could be retrieved from the Catia CAD model. Figure 9 shows a simplified model of the mechanical system before CAD geometry was imported.

Dokumentslag *Type of document*
REPORT-MSc. Thesis

Reg-nr *Reg. No*
AIF288-2-RE-0496

Infoklass *Info. class*
Öppen

Utgåva *Issue*
A

Sida *Page*
23 (56)
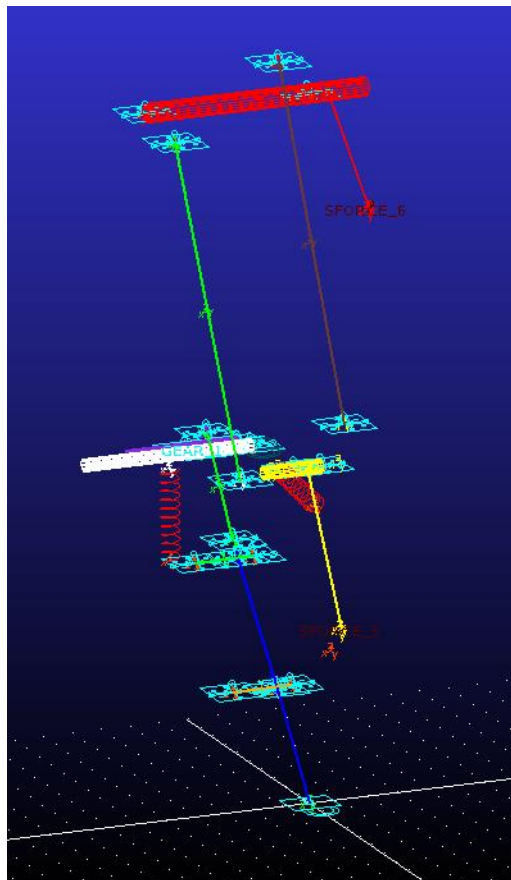
Figure 9. Simplified model of the mechanical system before CAD geometry was imported. The red cylinder is the shaft on which the inner handle is mounted on and the yellow cylinder is the shaft on which the outer handle is mounted on

3.1.2 Importing CAD geometry

In order to get more accurate mass properties of the parts in the model and to make the model look as the Saab engineers are used to see it, CAD geometry was imported to the model.

For the CED there already existed parts modeled in Catia. Assemblies of these parts could be saved as Step-files (*.stp/*.step) that could be import directly into MSC Adams. However, directly importing Step-files was not recommended by MSC since the result often were some parts not being imported as massive solids but as mass-less sheet-bodies instead. The reason why geometry turns into sheet-bodies instead of solids was that MSC Adams finds a hole or holes in the geometry and could therefore not make it a solid.

If the geometry was imported with the only purpose to be visual then some parts being sheet-bodies would not have made a difference. However, importing geometry as solids has advantages. If density was applied to an imported solid part then MSC Adams could automatically calculate mass, centre of mass and inertia for that part.

To increase the chances of receiving solids when importing geometry, the Step files from Catia were converted into MSC Adams preferred file format Parasolid (*.xmt_txt). With the CAD geometry in the file format Parasolid then the majority of the parts could be imported as solids. However the conversion from Step to Parasolid file format was done by third-party computer software. In this work the computer software Rhinoceros Inc [6] was used to convert Step files into Parasolid files. The mass for the parts still being imported as sheet-bodies were added to a nearby solid. In Figure 10 the entire mechanical system are shown with geometry from Catia.

Picture removed in published report due to Intellectual Property reasons
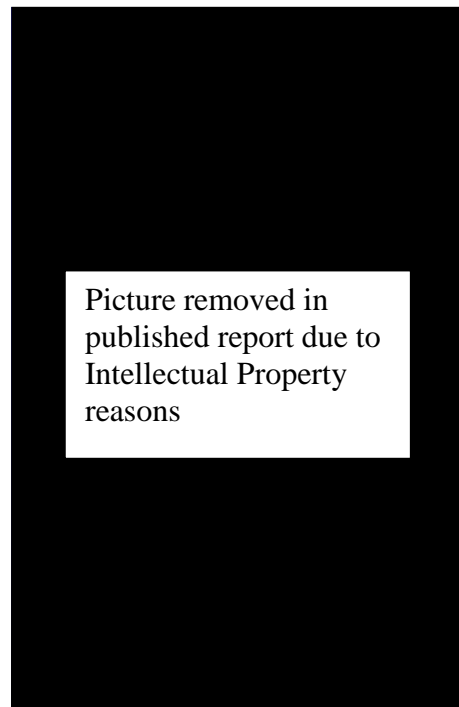
Figure 10. The mechanical system with CAD parts from Catia. In this figure the parts not belonging to the mechanical system has been made partly transparent

3.1.3 Accurate mass

In order to get the MSC Adams model to have accurate mass, one important thing was to import CAD parts for which MSC Adams calculated centre of mass and inertia. Mass for the parts in the mechanical system and the total mass for the door were set manually according to a CED mass data report, [10]. For the mechanical system attached to the fuselage (CB and jettison mechanisms) their mass was set to what MSC Adams automatically calculated when the parts were given a density.

The mass for the parts on the CED that did not belong to the mechanical system were added together to the door blade. The mass and the centre of mass were adjusted so the total mass and combined centre of mass for the door corresponded with CED mass data report, [10].

3.1.4 Redundant constraints

It is important to be careful when building a mechanical model. It is very easy by accident to lock a degree of freedom that is already locked by another joint. When this has happened the system is said to be over-constrained and the constraints causing it is called redundant constraints. An example of this could be a normal kitchen cabinet door. The door has two hinges and both constrain the door so it can not translate in any direction and only rotate around hinge line. This door is over-constrained since it basically would only require one hinge to restrain the door in that way.

However this is not a problem for the kitchen cabinet door since if there were a small misalignment in the hinges there would just be a small deformation at one or both of the hinges that would correct the misalignment. In rigid body mechanics however there exists no deformation so in the model of the same kitchen cabinet door there would instead be large forces between the hinges due to the misalignment. These loads have nothing to do with reality and therefore should over-constrained systems not be accepted in a rigid body model.

Fortunately there is a function in MSC Adams that, if the system is over-constrained, can calculate which joints are unnecessarily locking degrees of freedom. However it does not have to be that particular joint that is wrong. The function only states which joints are redundant.

An example of over-constrained bodies in the CED is the yoke. On the yoke three links are placed, see Figure 11. These links will together function as a parallelogram lifting the door with a stable motion.
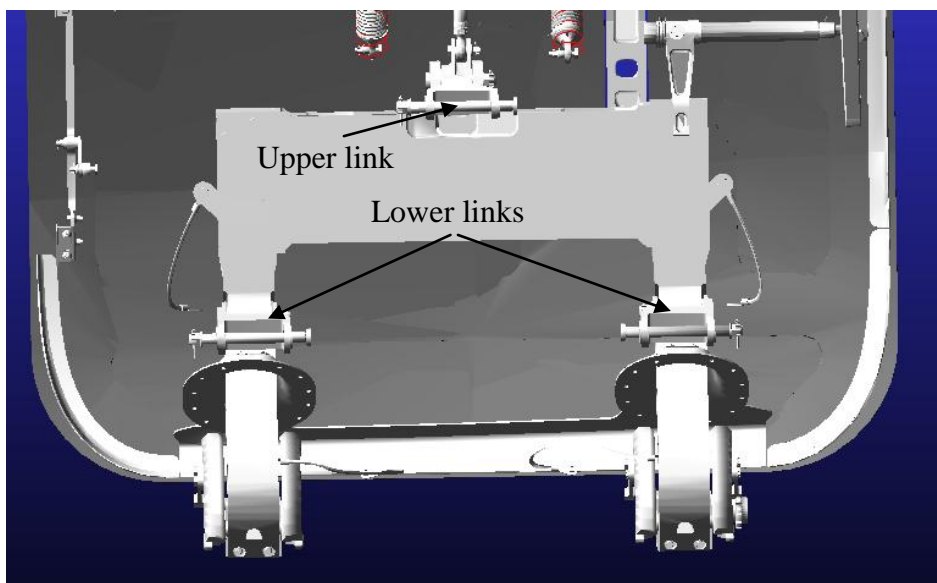
Figure 11. Yoke with upper link and lower links shown.

In the MSC Adams model the upper link was connected to the door with a spherical joint that locks all translations. It was the same thing for the lower link on the fwd side however on the aft side a spherical joint would create a redundant constraint in the direction between the two lower links. The solution would be to apply a joint that only locks two translational directions

perpendicular to a line between the lower links. Unfortunately no such joint exist, however by combining a spherical joint with a cylindrical joint than exactly that kind of a joint is created.

So therefore a dummy part was created and connected to the door with a cylindrical joint at the location for the lower link on aft side. At the same location a spherical joint connected the dummy part with the lower link. Consequently there were no redundant constraints.

3.1.5　　Modelling contact between bodies

In this subchapter it will be presented how the contacts were modelled, see 2.2.5 for more information on Contact functions.

3.1.5.1　　Upper Guide and Stop1

During the lifting manoeuvre, the Stop1 on fwd and aft sides are initially what keeps the CED from rotating outwards, see Figure 12 and Figure 13. Later in the lifting process a roller attached to the door starts to roll on a guide on both fwd and aft sides, see Figure 12. When this happens the Stop1 is no longer in use. When the roller has rolled over a cam on the guide then the door is free to rotate outwards, see Figure 14.
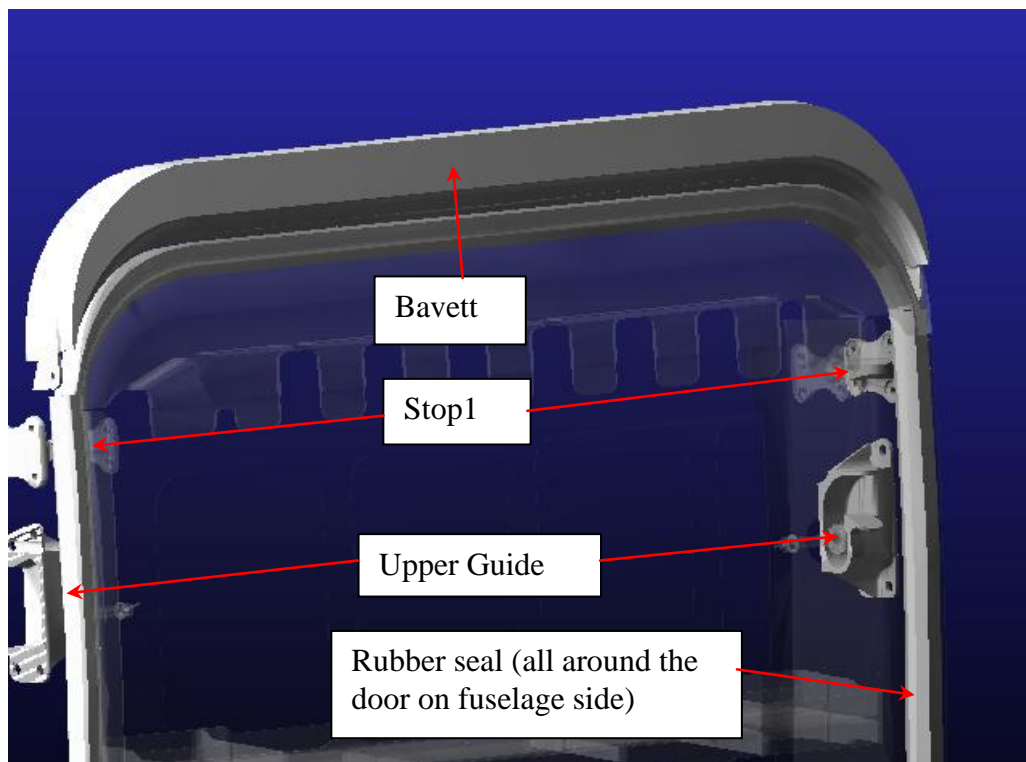
Figure 12. Bavett, rubber seal, Stop1 and Upper Guide (view from outside the aircraft)

The connection in Stop1 between the door and the fuselage was modelled using a Contact with Impact function. The stiffness was set to a value that gave a visually good contact i.e. small penetration. The damping values were set to standard values according to MSC Adams, [4].
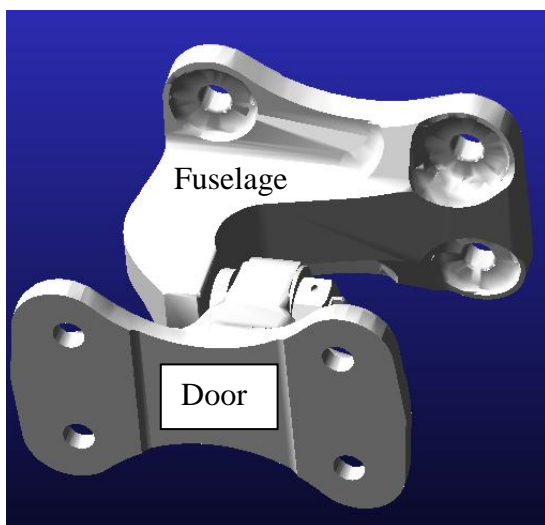
Figure 13. Stop1 on fwd side with the upper part being attached to the fuselage and the lower part being attached to the door
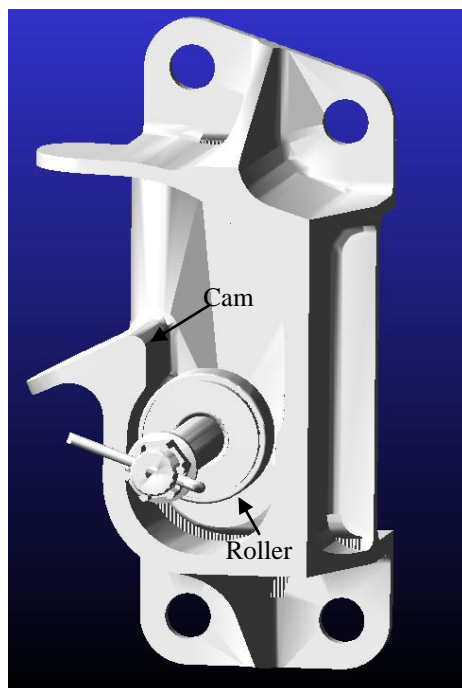
Figure 14. Upper guide on fwd side with cam (fuselage) and roller (door) pointed out

The connection between roller and Upper Guide were also modelled using a Contact with Impact function. The tricky part when modelling this contact was how to get a smooth contact between the solids since the forces varies a lot during the lifting manoeuvre. The results tended to be very spiky which required a lot of small adjustments to get an acceptable result. The stiffness could be lowered which gave much smoother results but that also gave greater penetration. The stiffness was ultimately set to a value that gave a visually good contact i.e. small penetration and no bouncing. The damping values were adjusted to achieve a smooth result.

Another method to model the contact was also tried where a spline (tubular data see 3.2.3) was created from the positions of a marker in centre of the roller. A curve attached to the fuselage (ground) could then be created from that spline. A dummy part could then be connected to the curve with a point-to-curve constraint and finally the roller was connected to the dummy part through a spring with variable stiffness.
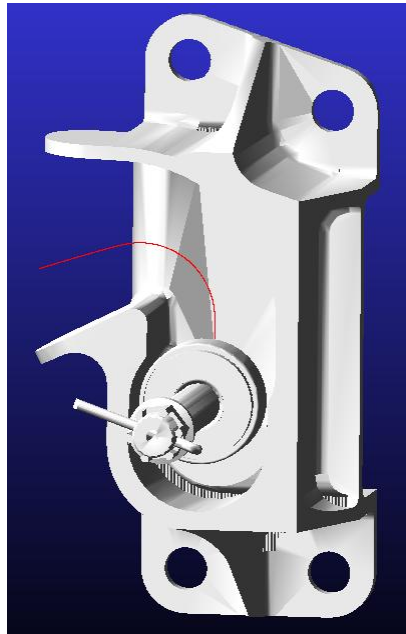
Figure 15. Upper Guide on fwd side with curve (red) from spline

The complexity of this method made the modelling of the connection very time-consuming. Before the connection was entirely finished, some simulations could already be done. These simulations showed results that were not any smoother than simulations with the Contact method. Risking more time-consuming modelling, a decision was made to use the Contact method for the Upper Guide connection.

3.1.5.2 Jettison lever

When pulling at the jettison handle, a little lever on shaft attached to the fuselage is pushing on a roller attached to a shaft on the door, see Figure 16.

Dokumentslag *Type of document*
REPORT-MSc. Thesis

Reg-nr *Reg. No*
AIF288-2-RE-0496

Infoklass *Info. class*
Öppen

Utgåva *Issue*
A

Sida *Page*
29 (56)
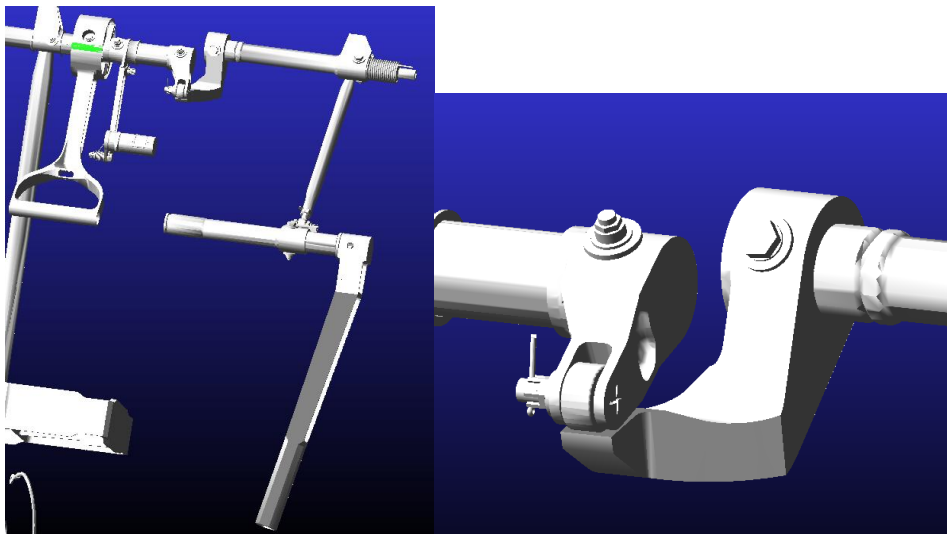
Figure 16. To the left there is the Jettison system and to the right there is a close up on the Jettison lever.

The shaft on the door side rotates by the forces from the jettison lever. Since the shaft on the door side is connected to the inner handle shaft, the rotation of jettison handle starts the lifting manoeuvre.

The connection between lever and roller was modelled with a Contact with Impact function. Stiffness and damping were adjusted until simulations showed visually real contact behaviour, i.e. small penetration and no large bounces.

3.1.6 Friction

At Stop1 friction were applied using the Contact with Impact function with the addition of a Coulomb friction. The coefficient of friction was obtained from reference [12].

Besides friction at Stop1, friction was also modelled between rubber seal on fuselage and sealing knifes on the door but also between bavett and door blade, see Figure 12 on page 26. There are no data given for the stiffness of the bavett, therefore it is assumed to be equal to the one for the rubber sealing (same assumption was done in the analytical method).

The rubber seal contact was modelled in two different ways. The first way was to model the contact with a Contact function, see 2.2.5, with the addition of Coulomb friction.

By adjusting stiffness, *k*, and force coefficient, *e*, a function was accomplished, see Figure 17, that corresponds to empirical data for the stiffness of the rubber sealing, [12].

$$F = kx^e$$

Where *F* is the contact force, *k* is the stiffness, *e* is the force coefficient and *x* is the penetration.
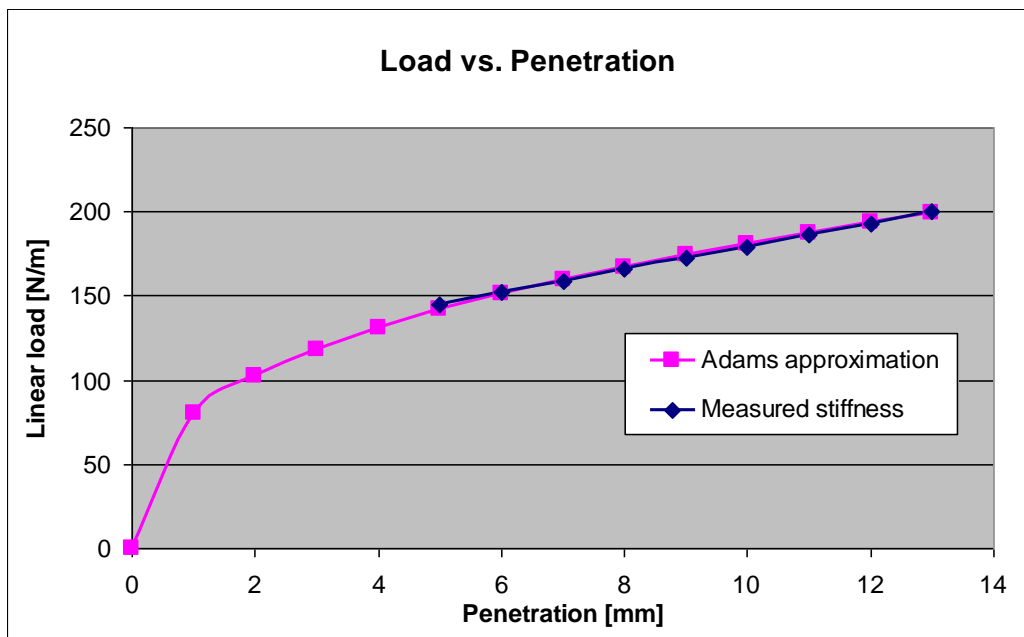
Figure 17. Load versus penetration for rubber seal.

The Coulomb friction, F_f, was calculated by multiplying a friction coefficient, μ_f, with the contact force, F.

$$F_f = \mu_f F$$

Using this method worked for Stop1, however it was shown that using a Contact function to model the contact at rubber seal was fundamentally wrong. The stiffness for the rubber seal was given as a line load versus penetration or in other words the force required to compress 1 metre of rubber seal a certain penetration distance. Simulation showed that the length of the contact was changing during the lifting manoeuvre and that caused a problem since in the built-in Contact function the contact force was not a function of the length of the contact.

In addition, simulations also showed that when using a Contact function there were not just one big intersection volume but instead several small ones. Every little intersection volume had then the stiffness of the entire rubber seal and consequently the friction force was highly overestimated. Since the number of intersection volumes was changing throughout the manoeuvre, the problem could not just be solved by dividing the rubber seal stiffness with the quantity of intersection volumes.

Instead a second method to model the rubber seal contact was created using several forces as a function of penetration. This method was basically a number of springs evenly distributed around the door and together they gave the stiffness for the entire rubber sealing according to empirical data, [12].
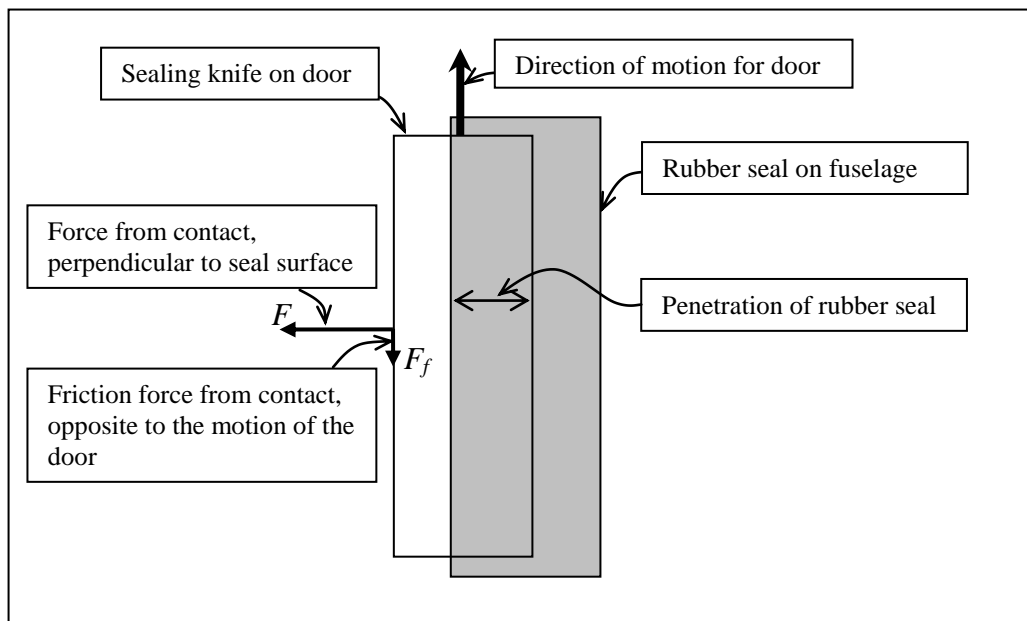
Figure 18. Sketch of the modelling between rubber seal on the fuselage and sealing knifes on the door

At first only three springs on either side was created where each spring had 1/3 of the stiffness for the rubber sealing. Thereafter the springs were increased to seven on either side where each spring had 1/7 of the stiffness for the rubber sealing for one side. Simulations with seven springs showed no big difference compared with simulations with three springs and therefore an assumption was made that no more springs needed to be added, engineering judgement.

This method coincides with MSC Adams help manual which states that when modelling collisions between very soft materials then the Contact function should not be used. According to the manual this should instead be modelled using forces, [4].

3.2   Applying loads on the model

In this chapter the loading condition and how the loads are applied on the model will be discussed.

3.2.1   Internal overpressure and aerodynamic damping

One of the load cases set by Airbus was to calculate how internal pressure (or outer suction) affect loads on components in the mechanical system during lifting of the door. Pressure can not be applied in MSC Adams instead it has to be replaced with a single force. Saab engineers had already recalculated the internal pressure to a force resultant [12]. The force from the internal pressure was applied in the MSC Adams model at a point called *Centre of Airload* (COA) [8]. The force from internal pressure was modelled so that when the door had been lifted and was starting to rotate outwards, the force was decreased to zero since the pressure difference then was assumed to level out.

Dokumentslag *Type of document*
REPORT-MSc. Thesis

Reg-nr *Reg. No*
AIF288-2-RE-0496

Infoklass *Info. class*
Öppen

Utgåva *Issue*
A

Sida *Page*
32 (56)

An aerodynamic damping force was applied to simulate the air drag during opening of the door. The damping was assumed to be a function of the angular velocity of the hinges, see Figure 2, [9].

$$F_{damping} = \frac{M_{damping}}{l_{coa}} = \frac{c \cdot \dot{\phi}}{l_{coa}}$$

Where M is the moment around the hinges, $F_{damping}$ is the load with the lever l_{coa} that creates the moment M, c is the damping coefficient and $\dot{\phi}$ is the angular velocity.

The damping has been modelled a force vector located in a point called *Centre of Airload* (COA) [8]. The orientation of the force vector was set by using a reference marker. The force vector is then oriented the same way as the reference marker during the simulation. The reference marker was in this case belonging to the part for the door blade and therefore would the force vector follow the door in its motion. An outcome of this is that the damping force and the force representing internal pressure could be directed perpendicular to the surface of the door during the entire simulation, see Figure 19.
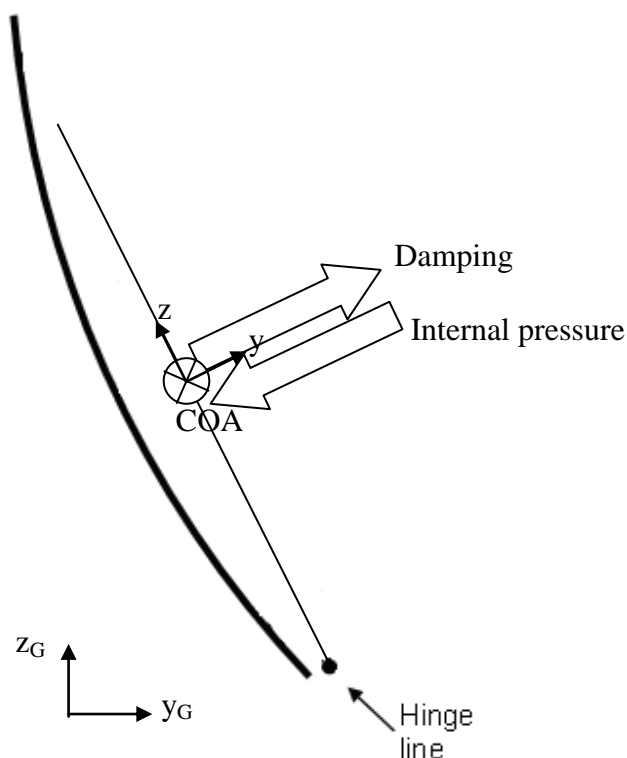
Figure 19. The system is following the door rotation.

The x direction of the force vector was in hinge line and the z direction was in the direction from hinge line to COA. Consequently the y-direction, which was the direction for the forces, was perpendicular to the hinge line and to the line between hinge line and COA.

3.2.2 Aerodynamic forces during Jettison

Airbus has decided that the CED should be able to jettison during high velocity flight with low altitude and with a high angle of attack. Saab has, with CFD software, calculated aerodynamic forces on the CED during these conditions for different opening angles. The aerodynamic forces were presented in a fix hinge line system, [9], see Figure 20.
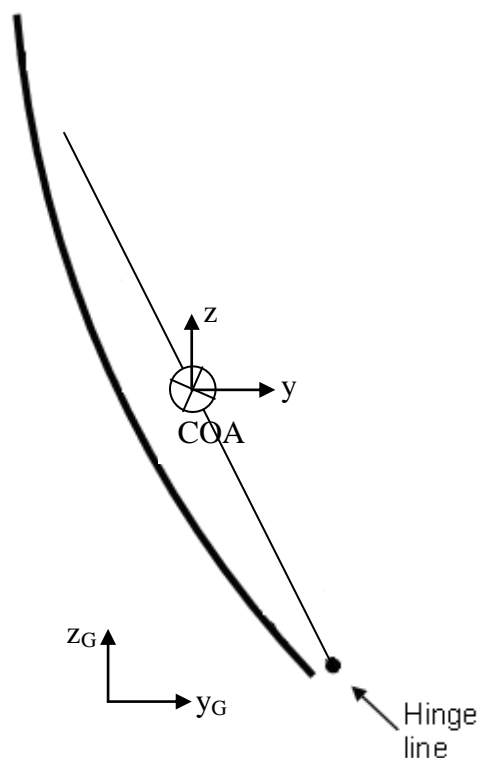
Figure 20. The fixed hinge line system was not following the door in its rotation

To apply the force vector for aerodynamic loads in the correct orientation, a reference marker added to ground was used. The reference marker was oriented such as the x-direction was in hinge line, z-direction was in global z-direction and y-direction was then perpendicular to both x- and z-direction.

In the result from the CFD analysis, the loads had been recalculated to be applied at hinge line instead of at COA with an effect of correcting moments. In the model the loads were placed in the COA resulting with that the correcting moments could be discarded.

3.2.3 Wind loads

Airbus has decided that the Crew Entrance Door for A400M should be able to be opened when subjected to wind loads in both opening and closing wind directions. Wind loads on the CED during opening have been calculated by Saab using FORTRAN software, [11]. The wind loads consist of forces in three directions and moments around those three axes for different opening angles of the CED. To simplify the managing of large amount of input data, the data was imported as splines.

Splines are tabular data and the benefit with working with splines is that it is possible to fit a function to the input data, see Figure 21. Functions were fitted to the input data using the Akima fitting method.
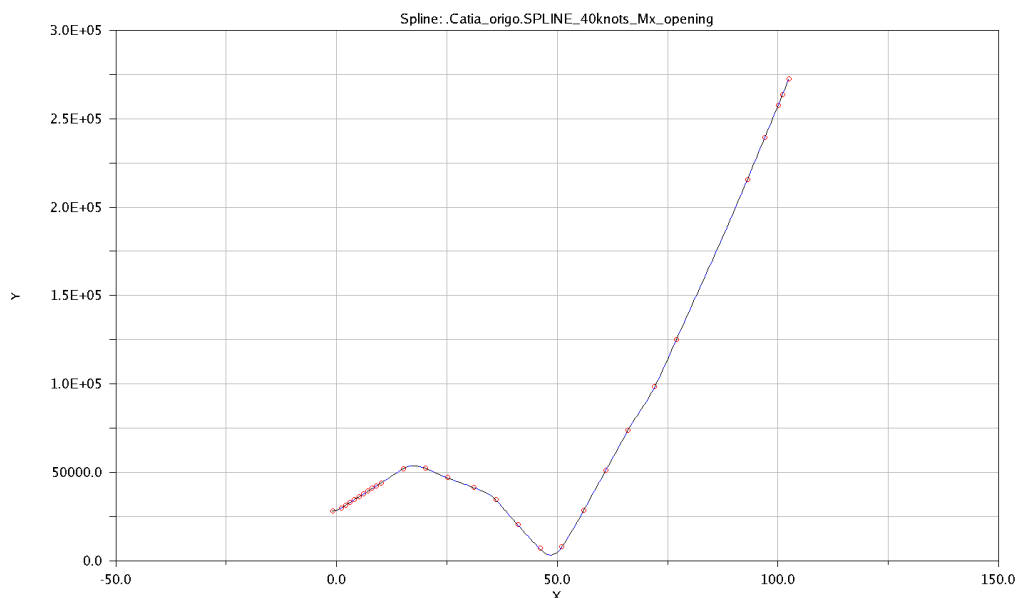
Figure 21. A Spline function (blue line) created from tubular data (red dots) with Akima fitting method. On the y-axis is the moment around hinge line and on the x-axis is the rotation of the hinges in degrees.

The functions were then implemented in a force vector with location at hinge line, between the two hinges.

To apply the force vector for wind loads in the correct orientation, a reference marker (added to the door) was used, see Figure 22. That way the force vector would follow the door in its rotation. The reference marker is initially oriented as the fix hinge line system (with x-direction in hinge line and z-direction in global z-direction) but is then rotated around the x-axis $\beta = \alpha_0 - 90$ degrees.

Dokumentslag *Type of document*

REPORT-MSc. Thesis

Infoklass *Info. class*

Öppen

Reg-nr *Reg. No*

AIF288-2-RE-0496

Utgåva *Issue*

A

Sida *Page*

35 (56)
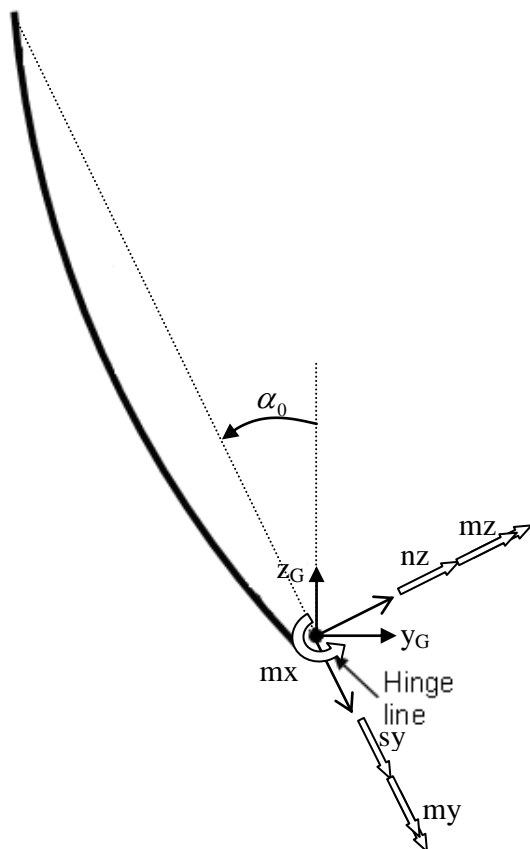
Figure 22. Aerodynamic ground loads system used in MSC Adams. The direction for tx and x_G was in aft direction along the hinge line.

3.2.4 Loads in opened position

In opened position the door also works as a staircase. One of the load cases was *one man running* and was basically a constant load in global z-direction applied on each step when in opened position. The positions for the loads were the same as in the analytical calculations, [11].

3.2.5 Handle loads

During lifting manoeuvre one of the external loads on the door was the handle load applied either on the inner or the outer handle in both opening and closing directions.

For example the inner handle load was calculated by first simulating lifting with all other external loads applied. A motion was applied on the inner handle shaft and the torque necessary to lift the door was measured. The values of the torque were divided by the lever distance and then imported as a spline to a force vector that was applied on the inner handle.

Thereafter a new simulation was made with the handle load applied and the torque was once again measured. The handle force would be sized perfectly if the torque would be zero at all times during the second simulation but since the handle force is an external force it changes the force equilibrium for the door.

Dokumentslag *Type of document*

REPORT-MSc. Thesis

Reg-nr *Reg. No*

AIF288-2-RE-0496

Infoklass *Info. class*

Öppen

Utgåva *Issue*

A

Sida *Page*

36 (56)

To minimize the torque values, the handle force were adjusted a few percent up or down.

4 RESULTS

In this chapter some results from the simulations of different load cases for the CED will be presented and compared to analytical results. Due to the large amount of result data only the most interesting results have been presented in this report while the other results have been moved to appendix A.

4.1 Lifting the door

To be able to open the door, it must first be lifted to a lifted position with either the inner, outer or jettison handle. Only results for lifting with inner handle is presented in this report. Results for outer handle and jettison handle are presented in appendix A. In the plots the forces are presented as functions of the Latch shaft rotation, see Figure 2. Zero degrees of Latch shaft rotation are equal to a closed and locked door while approximately 110 degrees of rotation represents a lifted position of the door.

Presented in Figure 23 are the handle loads necessary for opening the door the when not subjected to internal pressure.
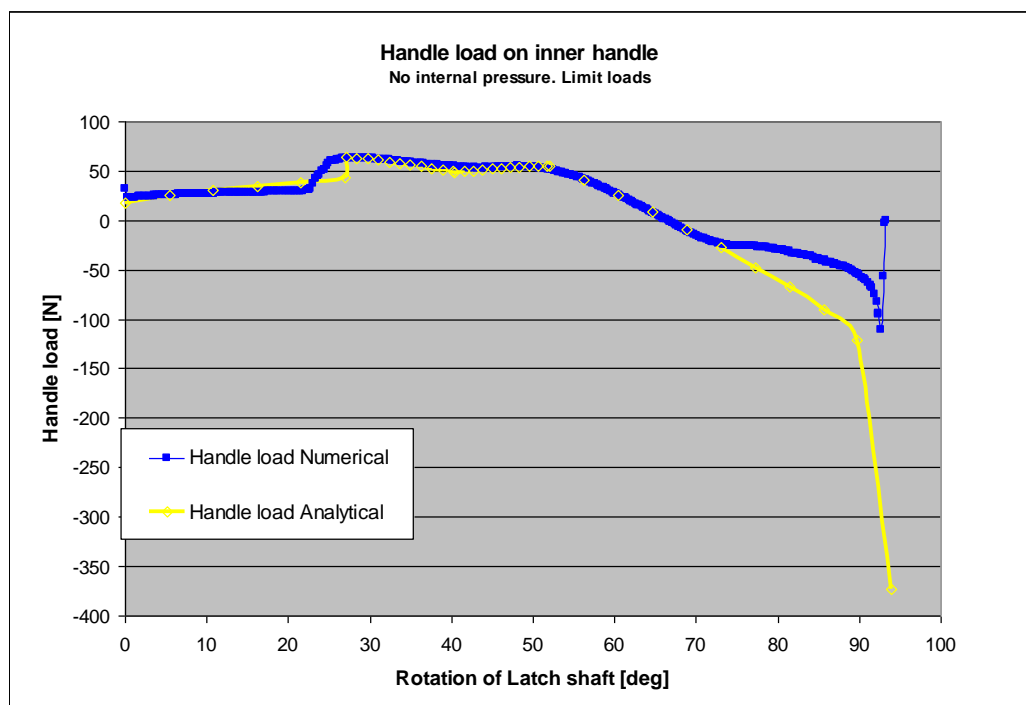
Figure 23. Necessary handle load on inner handle to be able to lift the door when not subjected to internal pressure

For handle loads it is basically only interesting with the values above zero, since negative values indicate that the mechanism then can lift the door by itself.

The numerical calculated maximum values of handle forces are similar to analytical calculations for all lifting cases. However, the numerical values increases rapidly at approximately 23 degrees of rotation of the Latch shaft as

the roller get in contact with the Upper Guide but in the analytical case the increase starts at around 28 degrees of latch shaft rotation. The five degrees corresponds to about 2 mm in lifting distance for the roller at Upper Guide, see Figure 24. This behaviour was noticeable for all plots concerning lifting and was an effect of a gap between the two sliding surfaces at stop1, modelled in the Catia geometry. In the analytical calculations it was assumed that Stop1 was in contact from the start. That was a correct assumption because when the CED is mounted on the fuselage then Stop1 is adjusted so there will be no gap.

However, in the MSC Adams model, the gap of 1.3mm, see Figure 24 and Figure 25, created an initial outward motion of the door. This resulted in the door ending up positioned slightly more outward in the numerical case then in the analytical case and therefore did the roller get in contact with the cam on the Upper Guide earlier, see Figure 26.
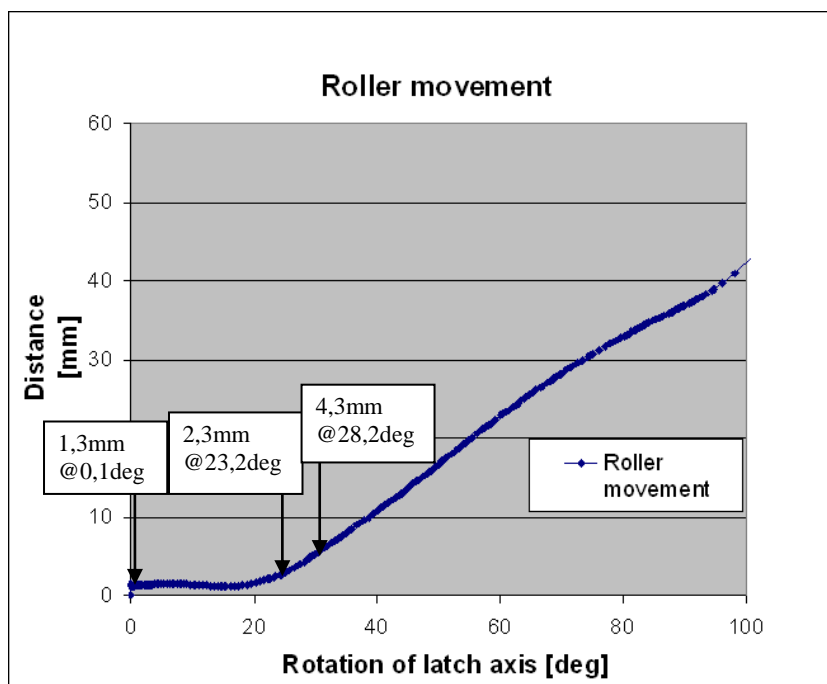
Figure 24. Movement of roller at Upper Guide
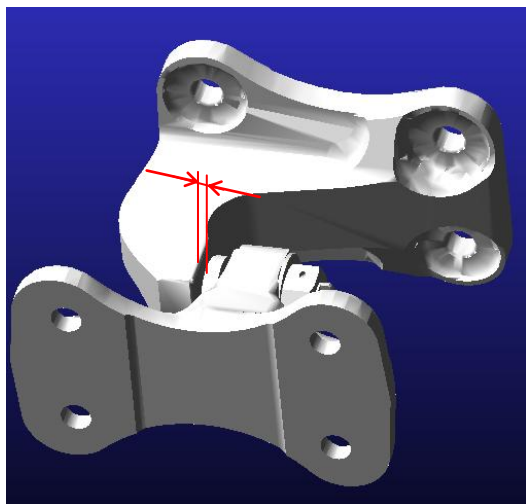
Figure 25. Gap at Stop1
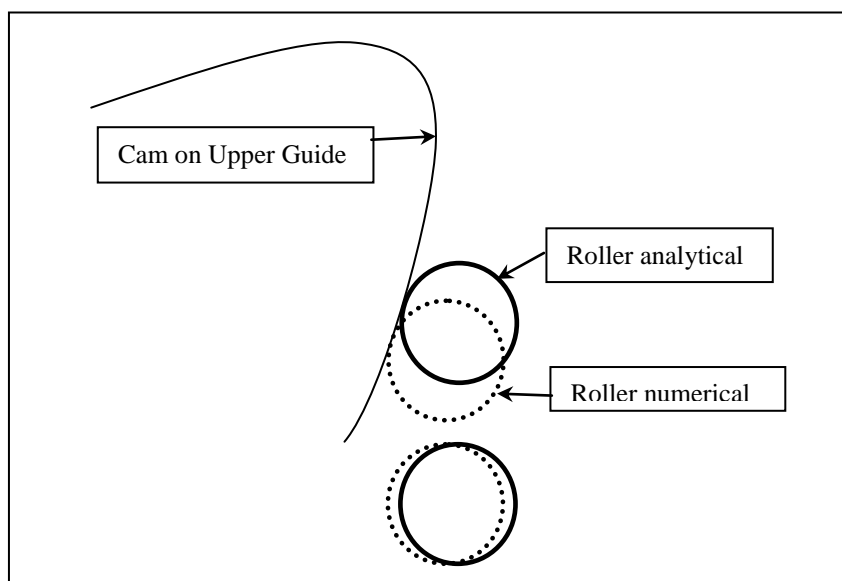
Figure 26. Exaggerated sketch of how the roller in numerical calculations
(dotted) gets in contact earlier with the Upper Guide than what the roller in
analytic calculations does (solid)

In Figure 27 the reaction forces in Stop1 and Upper Guide during opening with
inner handle are compared with analytical calculations. See chapter 3.1.5.1 for
location and purpose of Stop1 and Upper Guide.

	Dokumentslag *Type of document*	Reg-nr *Reg. No*
SAAB	**REPORT-**MSc. Thesis	AIF288-2-RE-0496
	Infoklass *Info. class*	Utgåva *Issue* Sida *Page*
	Öppen	A 40 (56)
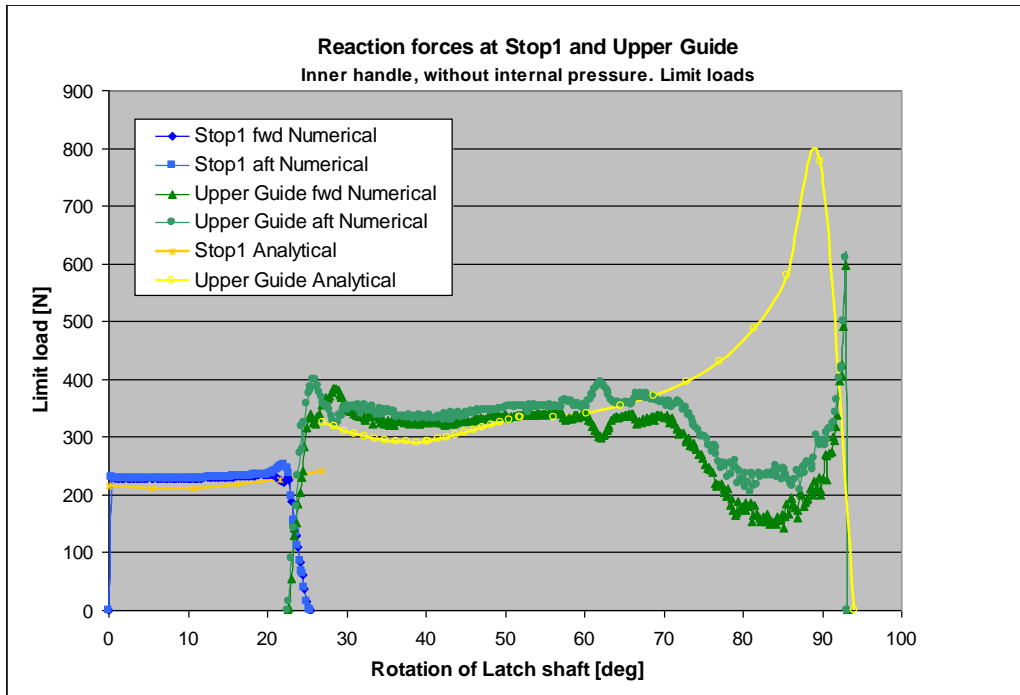
Figure 27. Reaction forces during lifting as a function of latch shaft rotation. No internal pressure applied. Fwd implies forward side hinge and aft implies hinge on after side. In the analytical case the forces were assumed to be the same for both sides

The results start to differ significantly for both inner handle loads, in Figure 23, and reaction forces at Upper Guide, in Figure 27, at about 70 degrees of Latch shaft rotation when the handle load gets negative. The differences were likely a result of making a dynamic model of the CED in MSC Adams instead of a kinematic model. The analytic calculations were based on a kinematic model which had a predetermined path for the roller on the guide. For every position of the roller on the path, a static calculation was made to get the forces necessary to maintain that position. However, in the dynamic model (in MSC Adams) there were no static calculations along a predetermined path. Instead the handles were rotated at a certain angular velocity and the forces and accelerations were deciding how the door was moving. In the case without internal pressure the upward directed acceleration of the door from the handle rotation was large relative the outward directed acceleration caused by gravity. Therefore are these simulations not similar to the analytical static calculations.

In Figure 28 the necessary handle load to lift the door with internal pressure applied is presented. In Figure 29 the reaction forces in Stop1 and Upper Guide during the manoeuvre are compared with analytical calculations.
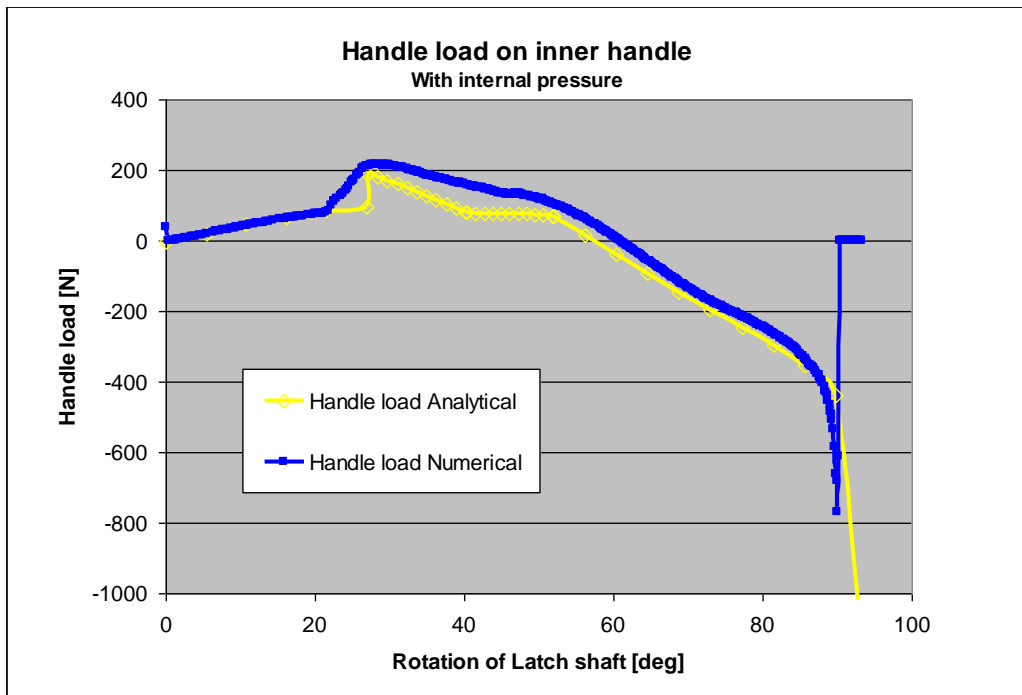
Figure 28. Necessary handle load on inner handle to be able to lift the door when subjected to internal pressure
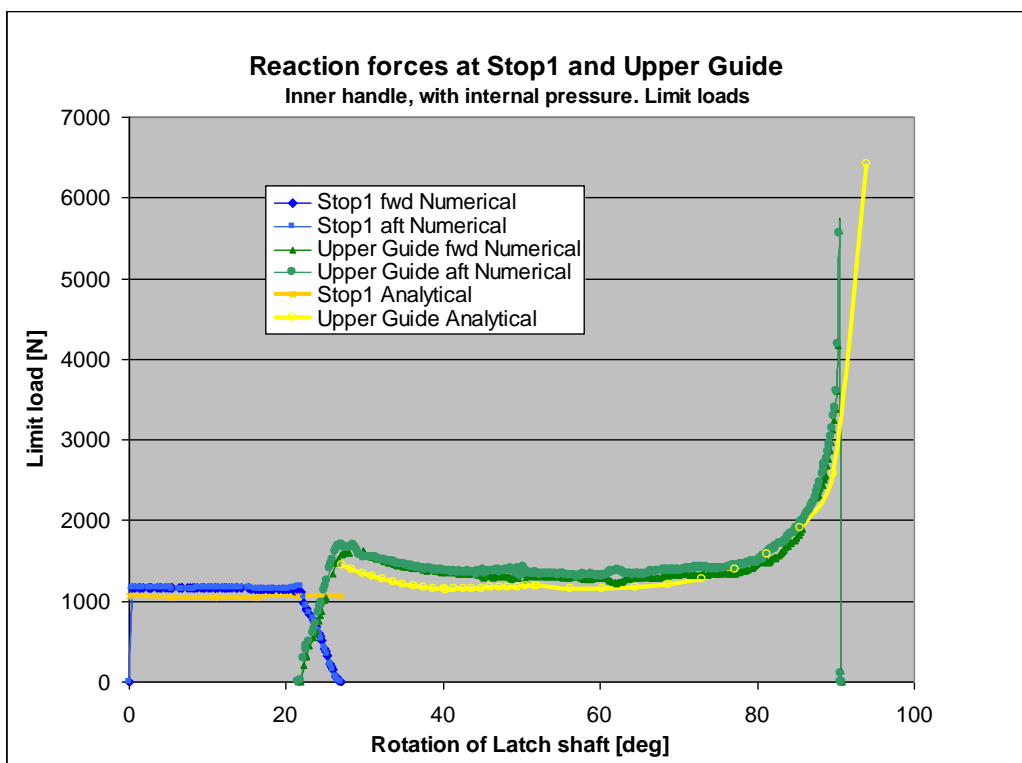
Figure 29. Reaction forces during lifting as a function of latch shaft rotation. Fwd implies forward side hinge and aft implies after side hinge. In the analytical case the forces are assumed to be the same for both sides.

In the case with internal pressure, the external force was pulling on the door creating an outward acceleration much greater than the upward directed acceleration. That together with the limitation of angular velocity of the inner handle made therefore that the simulation was more similar to a static

calculation. As a result, the reaction forces were more similar in this case than when internal pressure was not applied.

The top was not fully reached in Figure 29 and the cause of that was believed to be the Contact function used between roller and guide, see the discussion of the Contact function 5.2.

One simulation that could be done with a dynamic model but not with the kinematic model used in the analytic calculations was to lift the CED with the handles and then let go of the handles when the mechanism could continue the motion by itself, i.e. when the handle force otherwise would have been negative. The result from such a simulation with loads on inner handle is shown in Figure 30. Analytical values for lifting were added to the figure for comparison purpose.

Reaction forces at Stop1 and Upper Guide
Inner handle released at 58 degrees of latch shaft rotation, with internal pressure. Limit loads

Legend:
- Stop1 fwd Numerical
- Stop1 aft Numerical
- Upper Guide fwd Numerical
- Upper Guide aft Numerical
- Stop1 Analytical
- Upper Guide Analytical
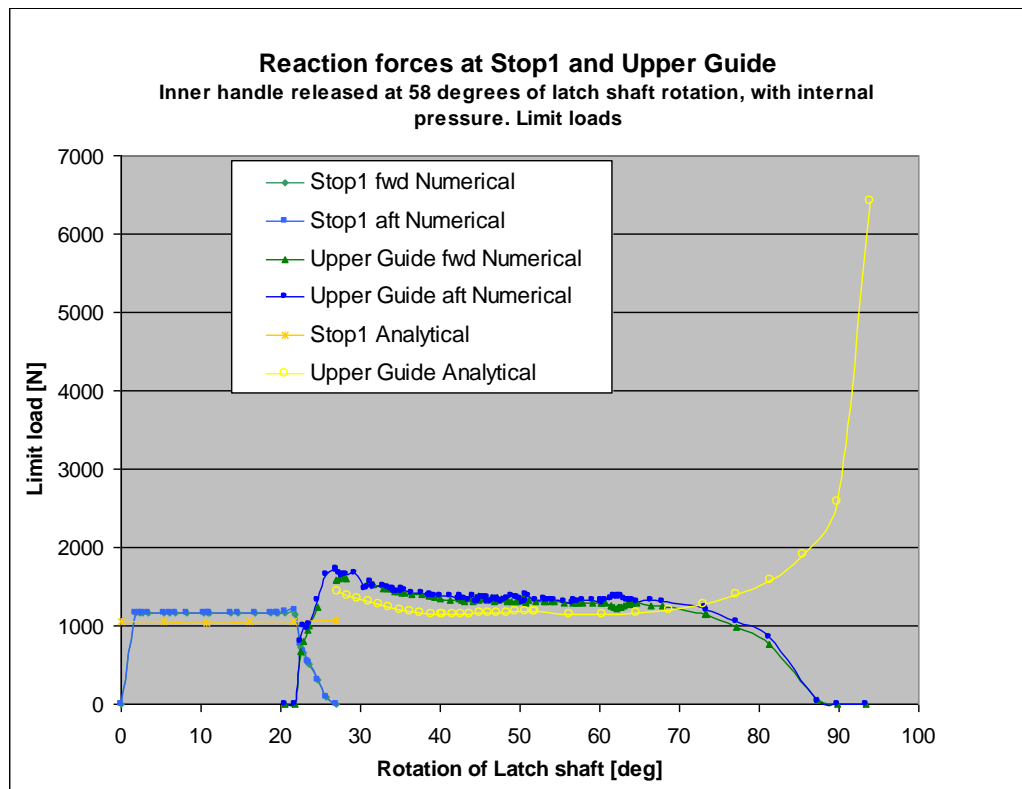
Figure 30. Numerical reaction forces at stop1 and upper guide when releasing the inner handle at a position where the mechanism can continue by itself. In the analytical calculations the inner handle was active during the entire manoeuvre

When releasing the handles at 58 degrees of rotation for Latch shaft the unlimited upward directed acceleration of the door decreases the reaction forces at Upper Guide.

4.2   Jamming during lifting manoeuvre

In Figure 31 a jam in the gearbox, see Figure 2, was created. The forces in rod P7P10, see Figure 2, were measured when applying a maximal force on outer handle, Figure 31, in either opening or closing direction. In the plots the forces are presented as functions of the Latch shaft rotation, see Figure 2. Zero degrees of Latch shaft rotation are equal to a closed and locked door while approximately 110 degrees of rotation represents a lifted position of the door.
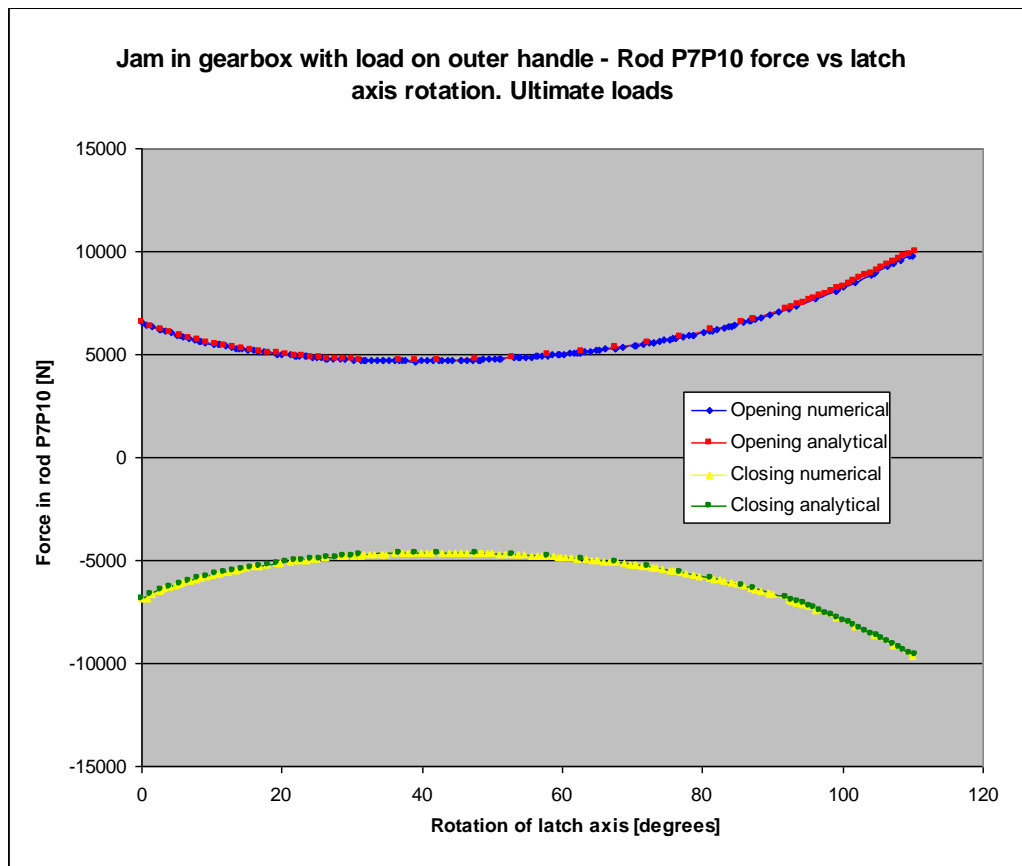
Figure 31. Force in rod P7P10 as a function of rotation of latch axis. Jam in gearbox and an ultimate force (1334N) was applied on the outer handle in either opening or closing direction

In Figure 32 the load in rod P2P6, see Figure 2, is presented during lifting when the force was applied on the inner handle and the jamming was at the outer handle. With no jamming in the gearbox the weight of the door contributes to the reaction forces in the rods. However in the analytical calculations the weight was neglected. To ensure that it was the weight that was causing the difference, some additional simulations of the MSC Adams model were calculated without gravity.
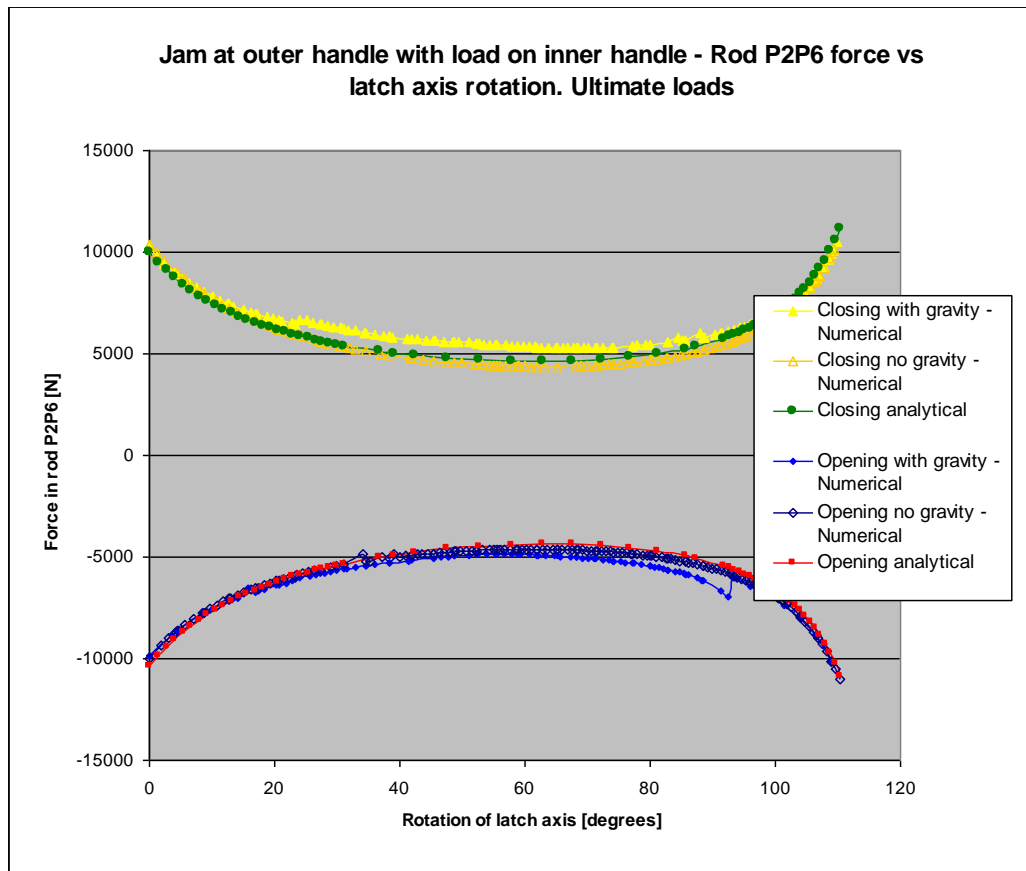
Figure 32. Force in rod P2P6 as a function of rotation of latch axis. Jam at the outer handle and an ultimate force (1334N) was applied on the inner handle in either opening or closing direction

In appendix A more reaction forces in rod P2P6 and rod P7P10 are presented.

4.3   Opening the door

After the door has been lifted it can be opened. The opening manoeuvre was controlled by a motion on the CB handle. The motion was programmed to open the door from lifted position in 4.8 seconds. The door was simulated without loads from wind but also with wind loads in both opening and closing directions. Only results with wind loads in opening directions are presented in this report since results for no wind and closing wind were similar to opening wind and was therefore moved to appendix A. In the plots the forces are presented as functions of hinge rotation, see Figure 2. Zero degrees of hinge rotation are equal to a closed door while approximately 102 degrees of rotation represents an opened position of the door.

Numerically calculated reaction forces at hinges during opening are compared to analytical calculations in Figure 33 and the reaction forces in CB rod are compared with analytical values in Figure 34.
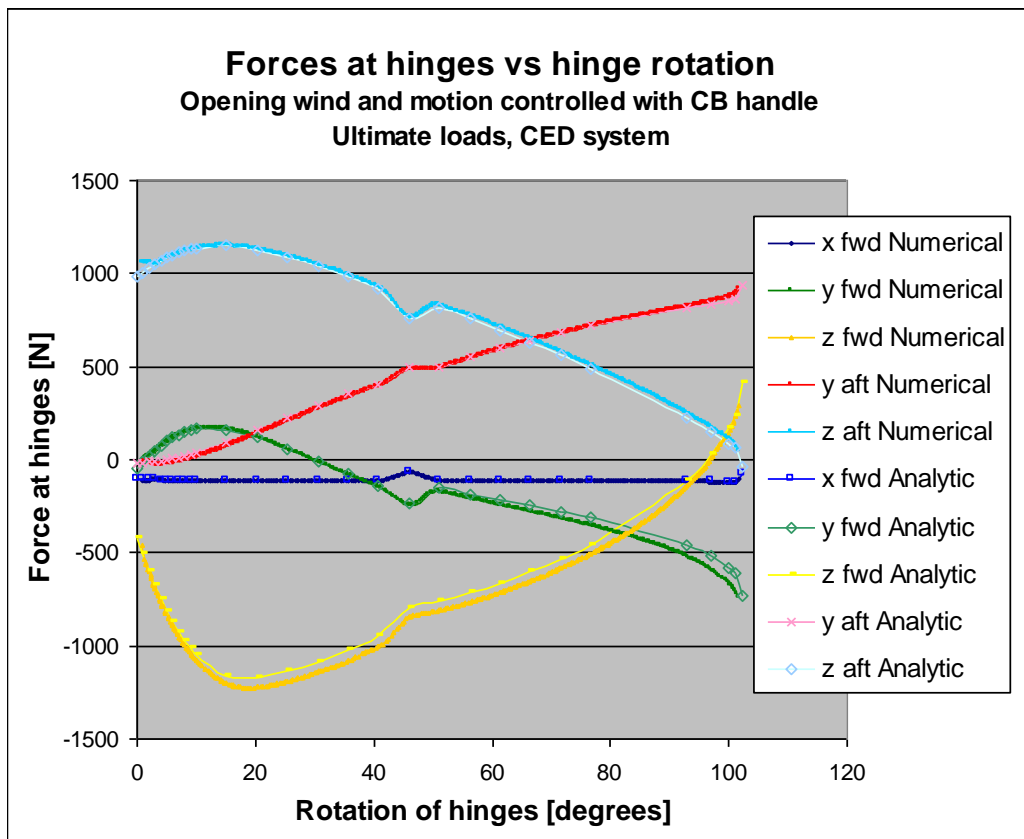
Figure 33. Forces at hinges during opening with wind loads in opening direction applied. Fwd implies hinge on forward side and aft implies hinge on after side. The movement of the door was controlled by a motion on the CB handle
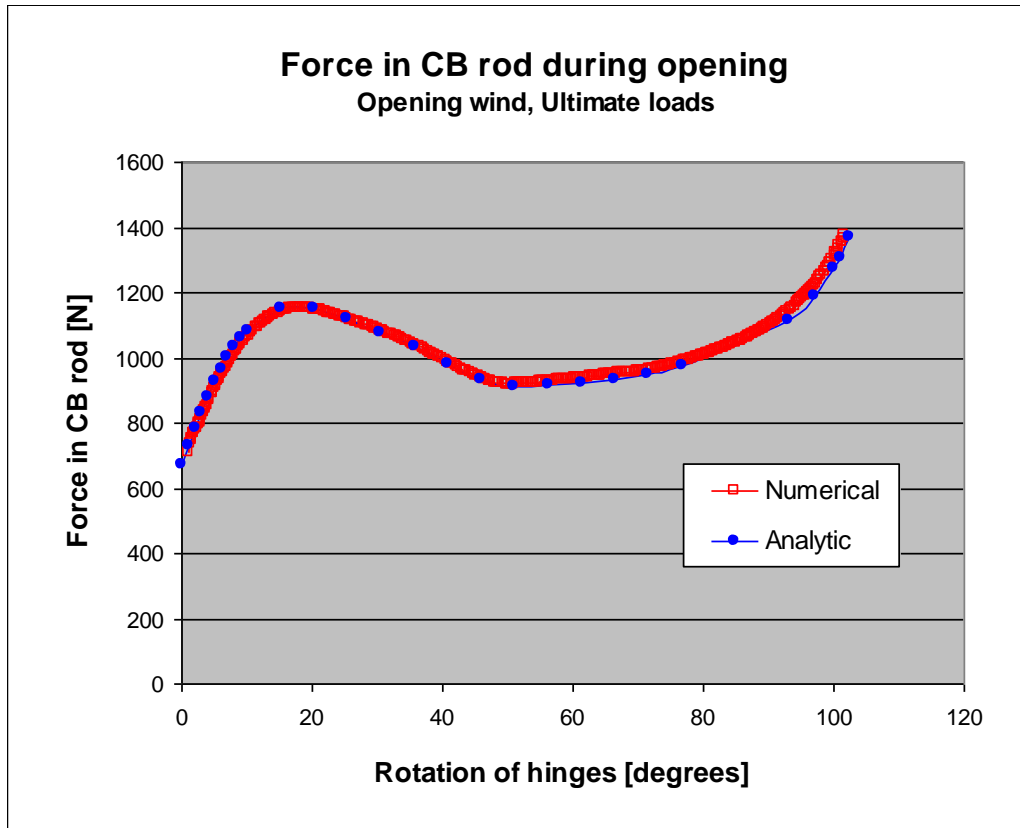
Figure 34. Force in CB rod when subjected to wind loads in opening direction

Both in Figure 33 and Figure 34 the results are very similar between numerical and analytical calculations.

4.4 Opened door

With the CED in opened position it works as staircase for the crewmembers. In Figure 35 the numerical calculated forces in the hinges for the case "one man running" are presented and compared to analytic results. For the same case reaction forces in the CB rod and in the wire, see Figure 3, were calculated. These reaction forces are presented in Figure 36 and Figure 37. In appendix A more reaction forces in several other load cases for opened door, see 1.5.4, are presented.
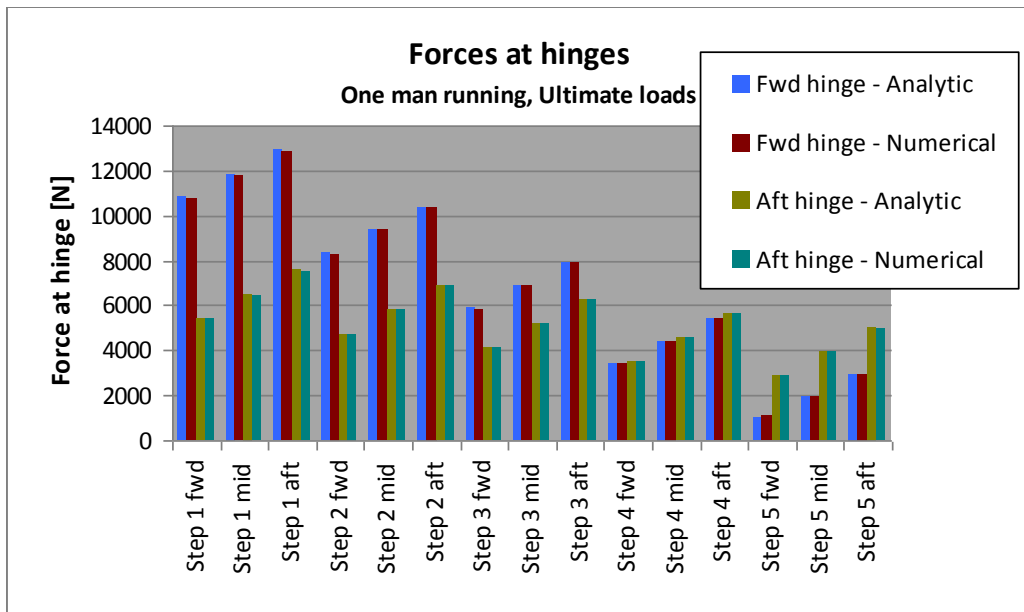
Figure 35. Forces at hinges in the case *one man running*. Three different positions to place the foot: fwd, mid or aft on each step

In Figure 35 the reaction forces at the hinges on both fwd and aft side are very similar between numerical and analytical calculations.
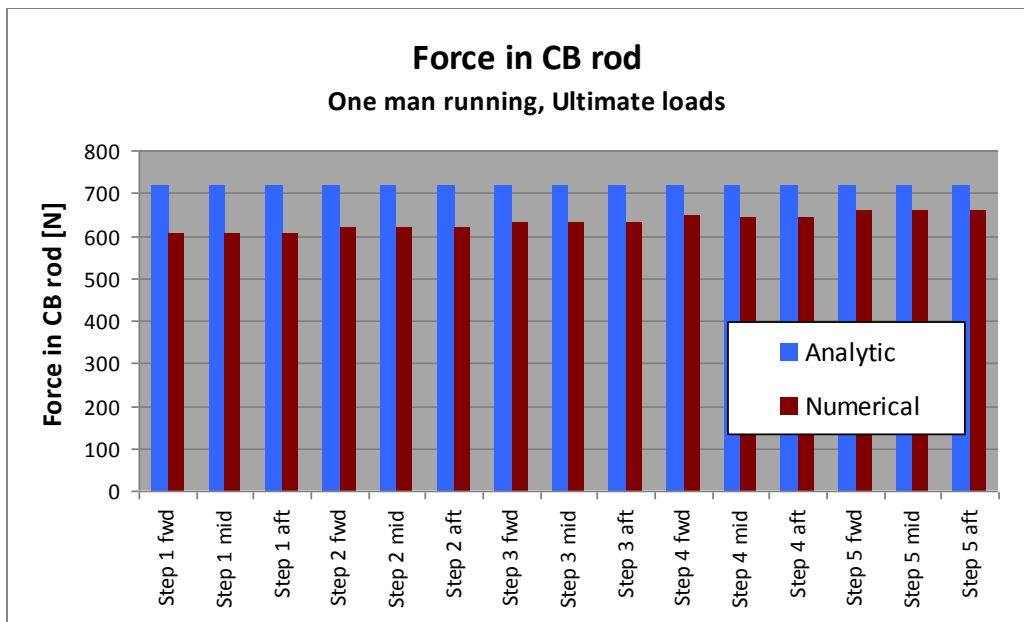
Figure 36. Forces in CB rod in the case *one man running*. Three different positions to place the foot: fwd, mid or aft on each step

In Figure 36 the numerical calculated reaction forces are not as big as the analytical values. This can partly be explained as a difference in mass for the CB rod and CB arm. In addition is the wire taking on more of the total force, see Figure 37.

	Dokumentslag *Type of document*	Reg-nr *Reg. No*
	REPORT-MSc. Thesis	AIF288-2-RE-0496
	Infoklass *Info. class*	Utgåva *Issue* Sida *Page*
	Öppen	A 48 (56)
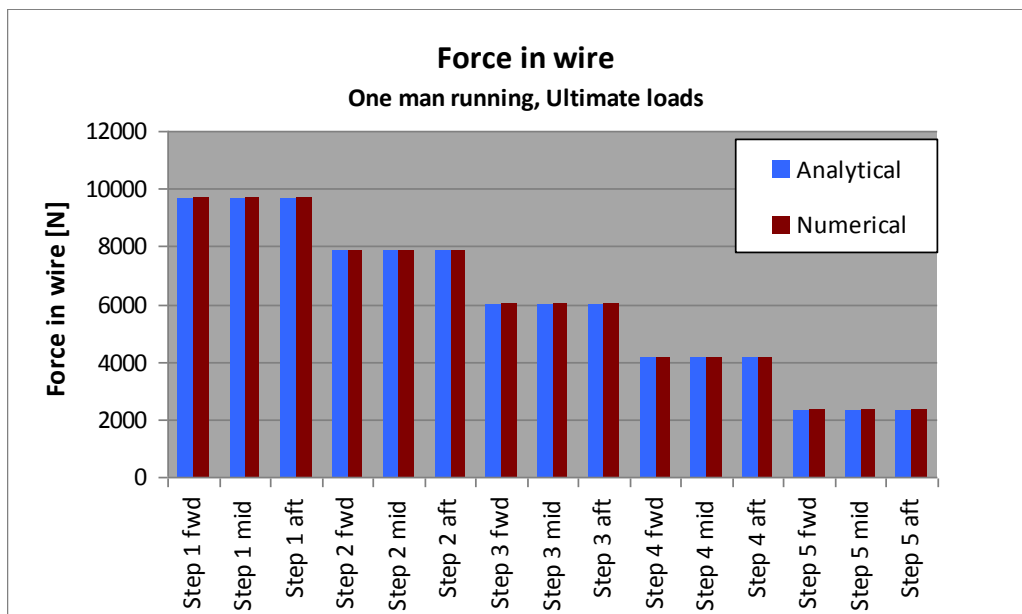
Figure 37. Force in wire in the case *one man running*. Three different positions to place the foot: fwd, mid or aft on each step

4.5 Jettison manoeuvre

The jettison manoeuvre disconnects the CB arm from the door and allows the CED to rotate outwards due to external aerodynamic loads. In the plots the forces and motions are presented as functions of hinge rotation, see Figure 2. Zero degrees of hinge rotation are equal to a closed and lifted door while approximately 113 degrees of rotation represents the position when the door was released from the aircraft.

In Figure 38 the motion of the CED during jettison is presented with velocity and acceleration of rotation for the hinges. In Figure 39 the reaction forces at hinges on both forward and after sides are presented as a function of opening angle (rotation of hinges).
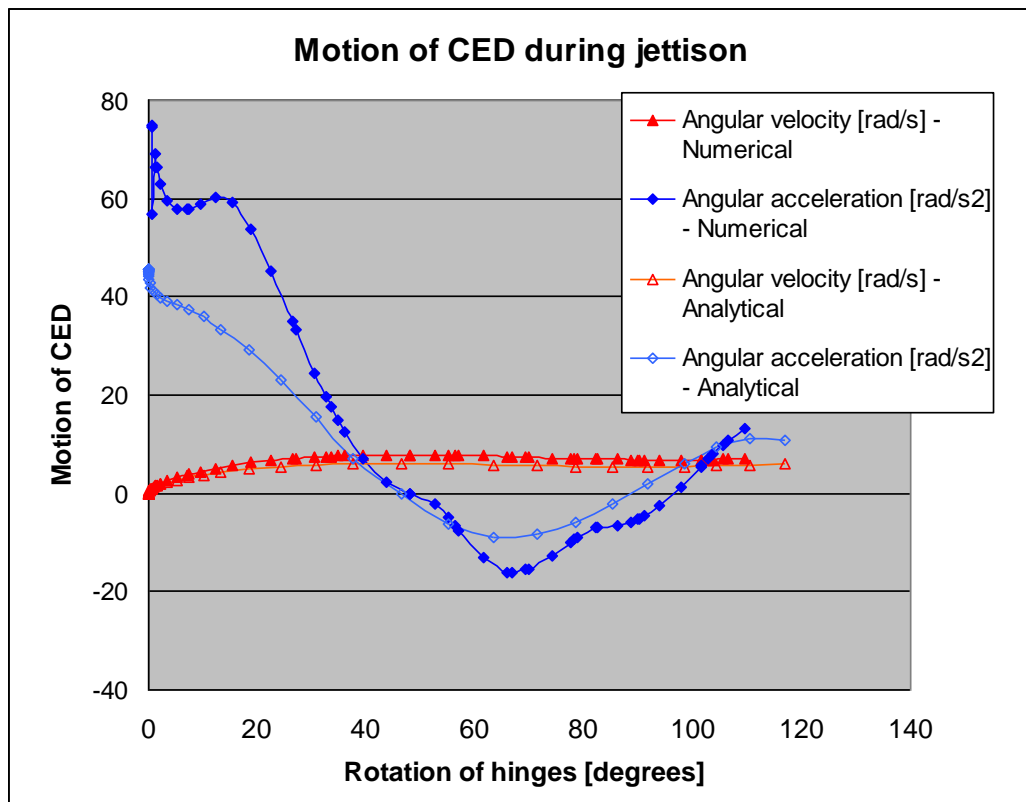
Figure 38. Motion of CED during jettison as a function of opening angle (hinge rotation)

In Figure 38 the acceleration values of the door differs between numerical and analytical calculations and that is likely a result of different inertia, see Table 1. The inertia for the MSC Adams model was less than for the analytical model in MS Excel and therefore were the angular acceleration higher initally for the MSC Adams model than for the MS Excel calculations.

Table 1 Comparison of inertia (around hinge line) for lifted CED

Analytic (MS Excel)	Numerical (MSC Adams)
79.61 kgm²	70.93 kgm²
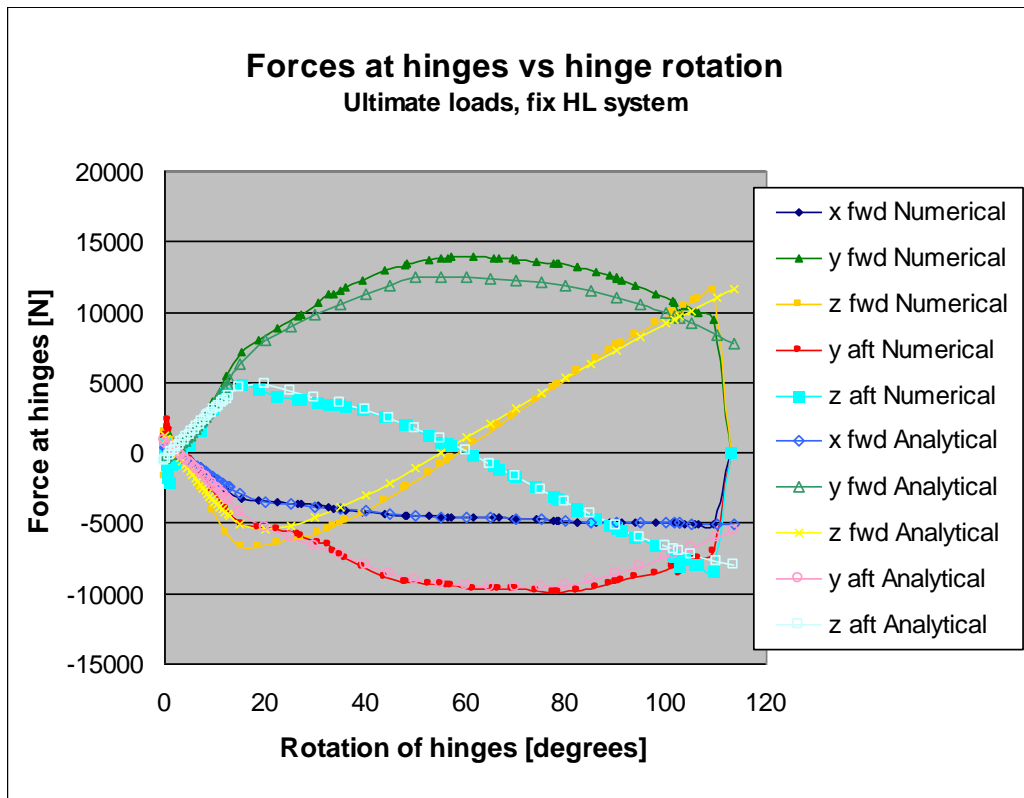
Figure 39. Reaction forces at hinges on both forward side and afterward side during jettison opening. Fwd implies forward hinge and aft implies hinge on after side.

5 DISCUSSION

In this chapter the *results* from the different load cases are discussed but also the use of *the Contact* function along with *mass accuracy* and *geometry import* are discussed. In addition the question of replacing future MS Excel calculation with MSC Adams calculations is also discussed.

5.1 Results

In this subchapter the results from different load cases are discussed.

5.1.1 Lifting the door

The difference between dynamic and kinematic models was shown when lifting without internal pressure. The CED was modelled as a dynamic model to simplify calculation of motion of the door during jettison. The idea was to get the dynamic model to be comparable with the analytical calculations by simulating the manoeuvres with a slow and constant angular velocity for the bodies in the system. However at lifting without internal pressure the small radius of the Upper Guide caused a difference between dynamic and kinematic calculations even though the angular velocity was less than 6 degrees per second for the rotation of the inner handle. When building these kinds of models it is therefore important to understand how the choice of model affects the results.

One advantage with the dynamic model was that it was possible to simulate what happens with the reaction forces when the handles are let go as soon as the mechanism could continue the motion by itself. Calculations for lifting with no negative loads were not possible to do with the kinematic model used in the analytical calculations. However this kind of simulation was probably more similar to reality than the other cases. In service it is not likely that the operator of the door would suddenly change its mind during lifting and start pulling in the handle with several hundred Newton. In the same way the dynamic model enables calculations of reaction forces during jettison after that the jettison mechanism is no longer in contact with the door.

5.1.2 Jamming during lifting manoeuvre

In Figure 31, with the jam in the gearbox, the results from the numerical calculations were very much alike those from the analytic calculations. However in Figure 32, with the jam at the outer handle, they differ in two ways. First of all a sign error in the analytical calculations had caused the numbers for opening and closing to switch place. Fortunately the numbers were very similar so it barely affected the results.

The other difference was that in the analytical case the weight of the door was neglected so therefore would the results differ. However in the same figure, Figure 32, a simulation with no gravity showed that it was gravity that created the difference.

Dokumentslag *Type of document*

REPORT-MSc. Thesis

Reg-nr *Reg. No*

AIF288-2-RE-0496

Infoklass *Info. class*

Öppen

Utgåva *Issue*

A

Sida *Page*

52 (56)

5.1.3 Opened door

For the case with one man running up the stairs, the numerically calculated values for forces at hinges, see Figure 35, was very similar to the analytical ones. This description is also accurate for hinge forces for the other cases with opened door, see appendix A.

However, the forces in CB rod differ between numerical and analytical values. The same type of results was found for the other load cases, see appendix A. In the load cases with opened door it is the wire that is taking the external load while the CB rod is only taking internal load from the CB spring. The difference is therefore not in how the loads were applied but instead how the CB mechanism was built and especially mass of the CB arm and rod. In the opening case it is the CB rod that is taking the external load and in those load cases the reaction forces were very similar. The reaction forces during opening are much higher than the forces in the opened cases and therefore can the difference in the opened case be neglected.

5.1.4 Jettison manoeuvre

In the jettison manoeuvre the difference in inertia, see 5.4, were shown as differences in angular acceleration, Figure 38. This might also be the reason to why the reaction forces at hinges differ slightly in Figure 39.

5.2 Use of the Contact function

The Contact function, see chapter 2.2.5, have been used to model a roller rolling on a cam at Upper Guide, see chapter 3.1.5, but also a contact at Stop1 and the jettison lever contact, see chapter 3.1.5.2.

The Contact with Impact function basically works as when two solids intersect each other, a spring is created trying to force them apart again. Equilibrium is reached when the force from the contact spring is equally large and opposite the force that is trying to push the solids together. However this means that equilibrium can only be reached when the two solid already has crossed each other surfaces. In the case with the roller and the cam at Upper Guide this means that the roller will get a slightly easier way over the top of the cam than in reality. In Figure 40 this effect is shown with a sketch.

Dokumentslag *Type of document*
REPORT-MSc. Thesis

Reg-nr *Reg. No*
AIF288-2-RE-0496

Infoklass *Info. class*
Öppen
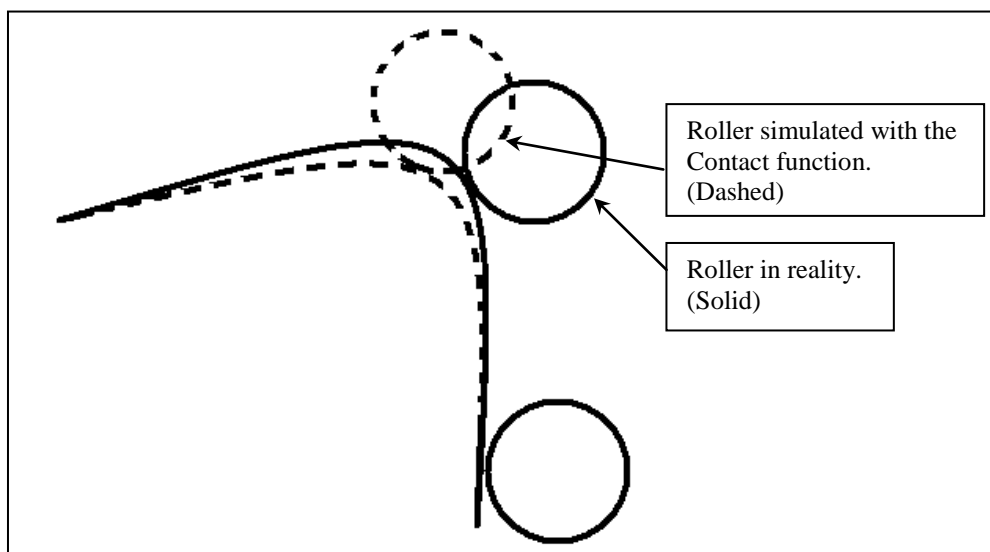
Utgåva *Issue*
A

Sida *Page*
53 (56)

Figure 40. An exaggerated sketch of how a Contact function simplifies the roller's path

The effect of the top being chopped off can be decreased by increasing the contact stiffness but that might instead cause more spiky results for the areas where the forces are smaller. One solution to this problem could be to adjust the model temporary according to what should be studied. If it is the area with the higher contact forces that are of interest and that the spiky result before this does not matter, then it is possible to increase the stiffness.

A version of this actually was tried for the Upper Guide. The method was to use a curve from a spline and a dummy part but as it turned out to be very time-consuming it was discarded, 3.1.5.1. However with this method it should be possible to use a spring with variable stiffness and create a contact that is a little bit softer when the forces are low and increases as the forces are getting larger.

5.3   Accurate mass

MSC Adams calculates centre of mass, mass and inertia for imported solids when they are given a density. For the CED model the mass was then adjusted to fit with Saab measurements [10]. However the centre of mass and inertia was not changed (except for the door blade part see 3.1.3).

An error that could arise here is when MSC Adams calculates the centre of mass it is assumed that the entire part has the same density but in reality these parts might be combined by parts of different materials and therefore different densities. For small parts this is probably negligible but for larger parts this might be something to think about.

	Dokumentslag *Type of document*	Reg-nr *Reg. No*
	REPORT-MSc. Thesis	AIF288-2-RE-0496
	Infoklass *Info. class*	Utgåva *Issue* Sida *Page*
	Öppen	A 54 (56)

5.4 Importing CAD geometry

Some geometry got imported as sheet-bodies instead of solids, see 3.1.2. One difference between sheet-bodies and solids is that sheet bodies are not given any mass, centre of mass or inertia when given a density. The effect of some parts not having correct inertia was shown in simulations such as jettison manoeuvre.

The reason why some geometry is imported as sheet-bodies is that they contain a hole somewhere on the surface. There exist software that can repair damaged parts and turn sheet-bodies into solids, for example Rhinoceros [6] and Ansa [7].

5.5 Replacing MS Excel with MSC Adams

The benefit of working with MSC Adams instead of MS Excel is that it is quicker and more user friendly. In addition, MSC Adams provides an extra immediate checking feature by animating the movement of the parts. Many of the built-in errors in the model configuration are therefore easily found and corrected.

Apart from calculating reaction forces and motions, MS Excel has been used to select critical values from the calculations and creating critical envelopes to use when sizing parts in the mechanical system. These post-simulation calculations seem not to be suitable to conduct in MSC Adams. They and other post calculations are in the Authors opinion probably best to keep doing in MS Excel. Results can be exported from MSC Adams in several ways, for example as tables that can be copy into MS Excel.

Another calculation that was made analytically in MS Excel was to calculate the bending moment of shafts at particular locations, for example if a there was a hole for a bolt. These bending moments can be calculated with the MSC Adams model by splitting the shaft in two (at the location of the hole) and placing out a fix joint that connects both sides of the shaft. Then the bending moment could be measured during simulation and presented in a coordinate system that follows the shaft in its rotation.

In addition, when starting a new project it must be able to bring the computer with software to another location, perhaps even to another country for a few months. This set demands on software licenses that can be mobile. According to a software specialist[1] at Saab the MCS Adams licenses will not be a problem.

---

[1] *Krus, Jonatan*, jonatan.krus@saabgroup.com, OOIDCA

6 CONCLUSION AND FUTURE WORK

Creating a model of a mechanical system in MSC Adams/View is easy and fairly quick. The benefit of working with MSC Adams instead of MS Excel is that it is quicker and more user friendly.

It is in the Authors opinion that for future projects, the analytical method with MS Excel to calculate reaction forces and motions of the CED can and should be replaced by numerical calculations with MSC Adams/View. The major differences in results between the two methods are believed to be an effect by comparing results from a kinematic model with results from a dynamic model and therefore not an effect of comparing analytical and numerical calculated values.

However, apart from calculating reaction forces there are additional post-simulation calculations for which it is perhaps more beneficial to use MS Excel. This is not a problem since MSC Adams can export results efficiently.

If Saab Aerostructures decides to start working with MSC Adams/View and if Saab wants geometry to be imported to the model, then a strong advise from the Author is to have a software installed that can convert step-files (*.stp or *.step) to the MSC Adams preferred file format Parasolid (*.xmt_txt or *.x_t). The software should also be able to repair geometry which will greatly increase mass accuracy.

A few things that can be continued to work with on this model are the contact on the Upper Guide and the releasing mechanism of the hinges during jettison. In addition, repairs of parts that have been imported as sheet-bodies can be conducted and thereby giving a more correct inertia to the model.

7   REFERENCES

[1] Airbus Military, http://www.airbusmilitary.com, [cited: 120426]

[2] Hoyle, Craig (2011). A400m on track for early 2013 delivery says airbus. *Flight global,* http://www.flightglobal.com/news/articles/a400m-on-track-for-early-2013-delivery-says-airbus-356937/, [cited: 120426]

[3] Christensen, Peter ( ). *Computational Rigid Body Mechanics,* Division of Mechanics - University of Linkoping, Unpublished course material for the course *Robotics and Multibody Dynamics*

[4] MSC Adams, *MSC Adams/View help* – 2012

[5] MSC Adams, *MSC Adams Solver help* – 2012

[6] McNeel, *Rhinoceros Inc –*,
      Webpage: http://www.rhino3d.com/, [cited: 120503]

[7] BETA CAE Systems S.A, *Ansa –*
      Webpage: http://www.beta-cae.gr/ansa.htm, [cited: 120503]

Saab internal reports:

[8] Saab AB, *A400M Crew Entrance Door – Load analysis for jettison –* AIF288-2-RE-0017 issue: F, Internal report

[9] Saab AB, *A400M Crew Entrance Door – External airloads and movement during jettison –* AIF288-2-RE-0122 issue: B, Internal report

[10] Saab AB, *A400M CED. Mass data for MSC Adams model –* AIF288-2-PM-0064 issue: B, Company restricted

[11] Saab AB, *Door CounterBalance Mechanism,* Static Justification report– 112502-M021BRP101291, Company restricted

[12] Saab AB, *A400M Crew Entrance Door – Calculation of handle and interface loads for door opening –* AIF288-2-RE-0099 issue: D, internal report

APPENDIX A

Lifting the door

Forces for when the door was simulated to be opened with the outer handle are presented in Figure 41 to Figure 44. The necessary handle loads to lift the door are presented in Figure 41 and Figure 42, respectively with and without internal pressure. In Figure 43 and Figure 44 the reaction forces at Stop1 and Upper Guide are presented and compared to analytical values, also here respectively with and without internal pressure.
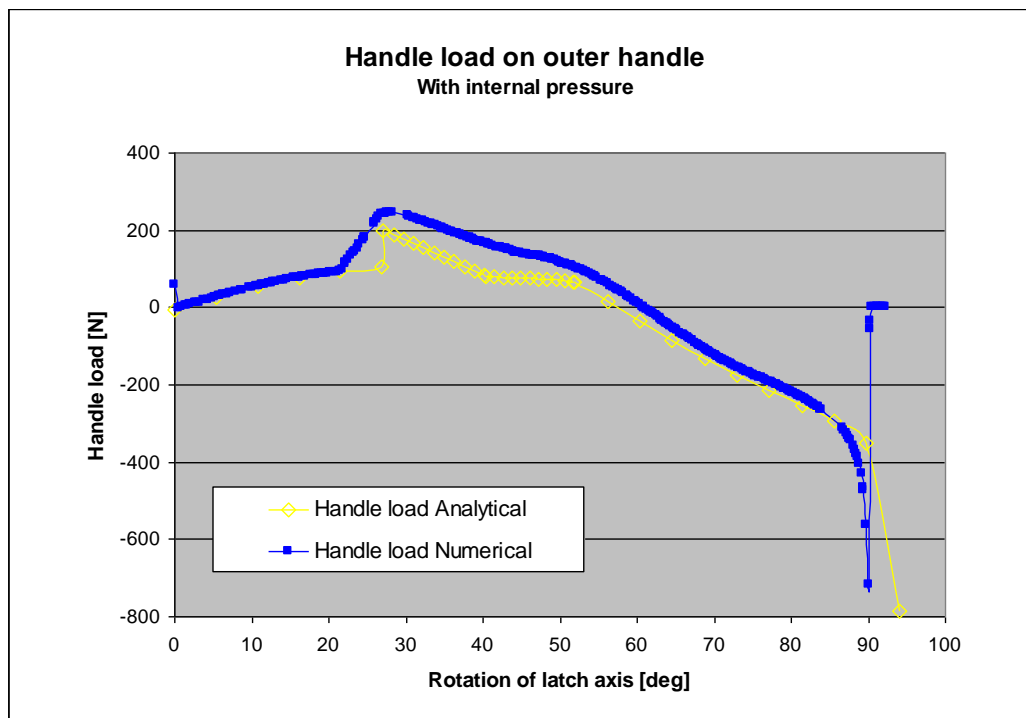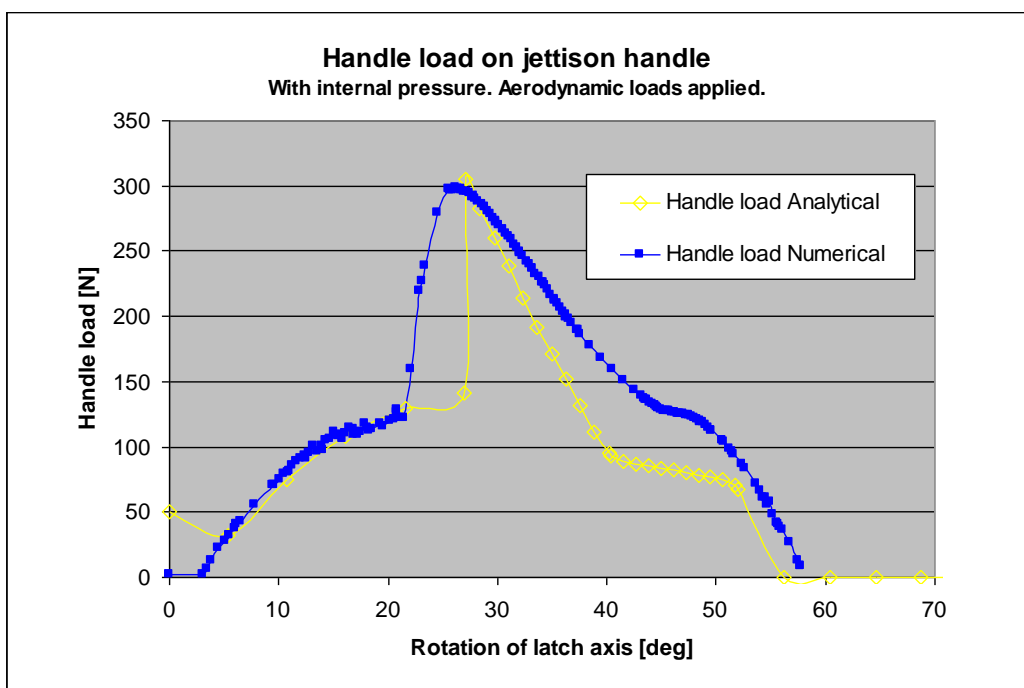
Figure 41. Necessary handle load (limit) on outer handle to be able to lift the door when subjected to internal pressure
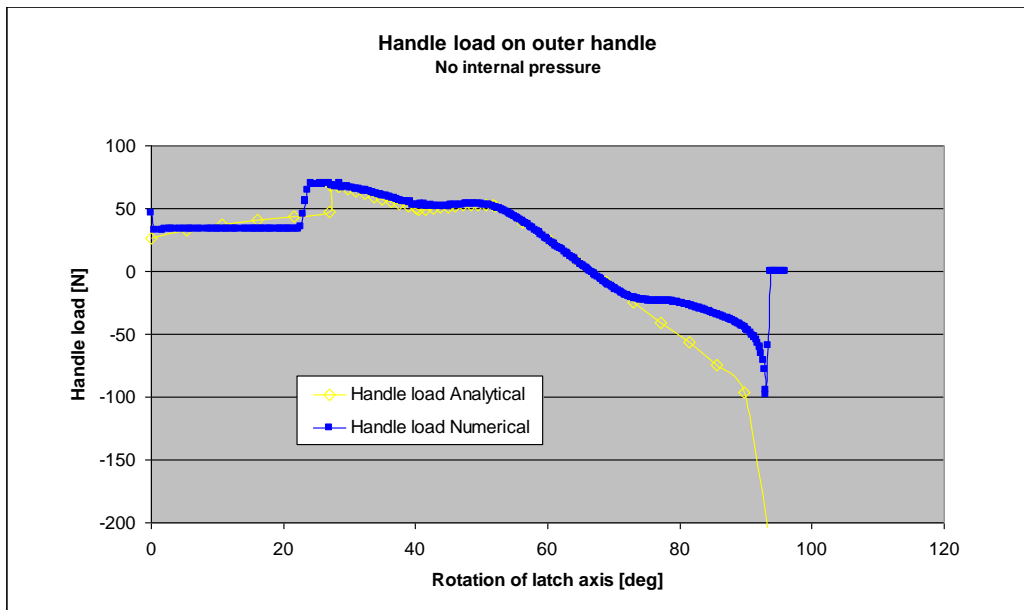
Figure 42. Necessary handle load (limit) on outer handle to be able to lift the door when not subjected to internal pressure
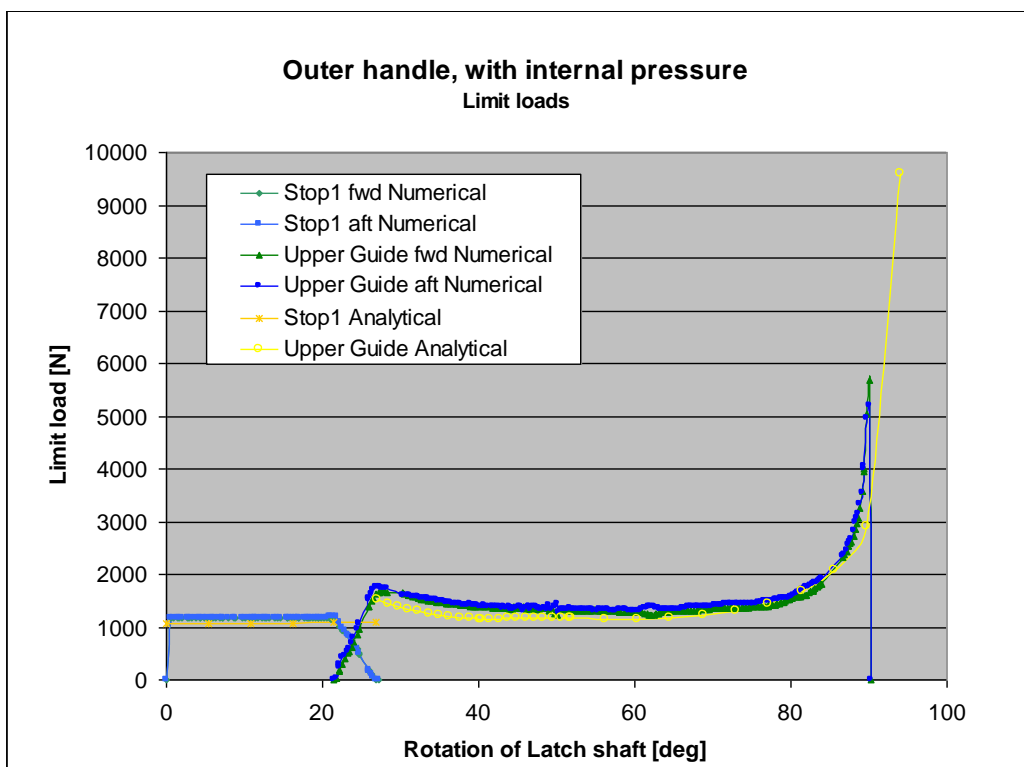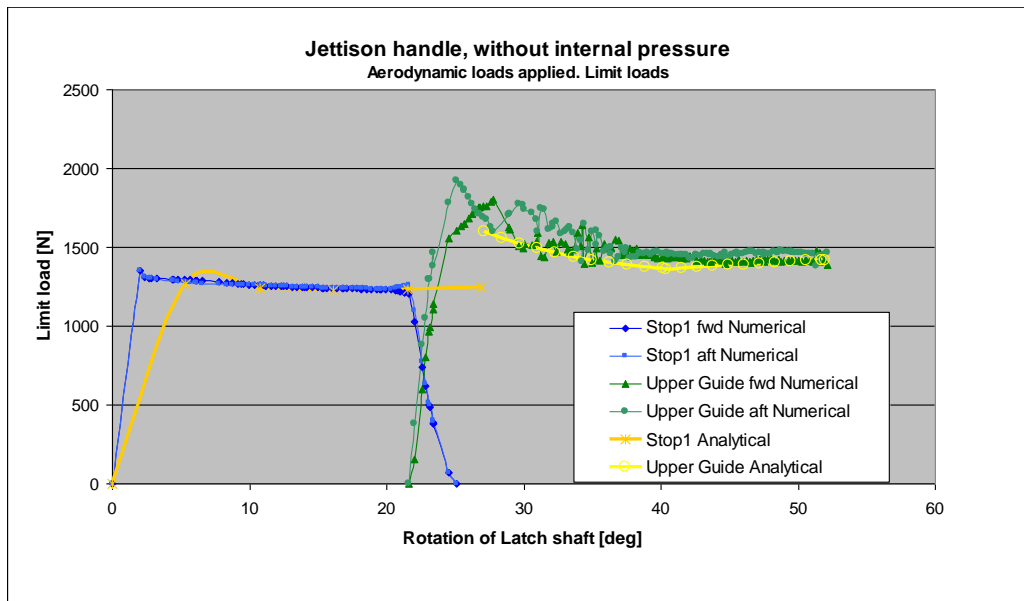

Figure 43. Reaction forces during lifting as a function of latch shaft rotation. Fwd implies forward side hinge and aft implies after side hinge. In the analytical case the forces are assumed to be the same for both sides
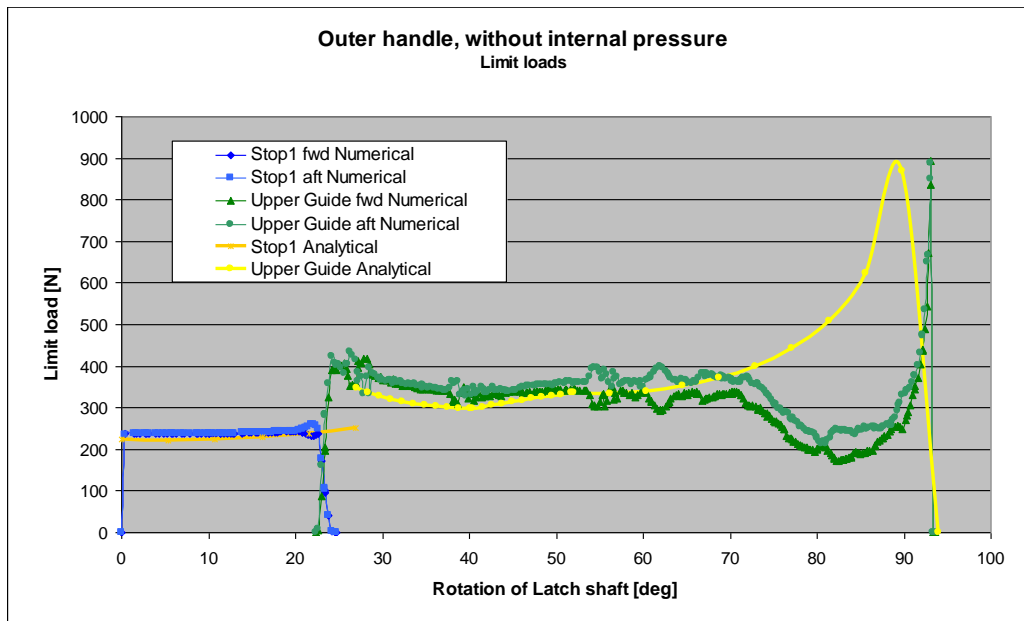
Figure 44. Reaction forces during lifting as a function of latch shaft rotation. Fwd implies forward side hinge and aft implies after side hinge. In the analytical case the forces are assumed to be the same for both sides

In Figure 45 to Figure 48 the door was lifted with the jettison handle and aerodynamic forces was applied on the model. The necessary handle loads to lift the door are presented in Figure 45 and Figure 46, respectively with and without internal pressure. In Figure 47 and Figure 48 the reaction forces at Stop1 and Upper Guide are presented and compared to analytical values, also here respectively with and without internal pressure.

Figure 45. Necessary handle load (limit) on jettison handle to be able to lift the door when subjected to internal pressure and aerodynamic loads
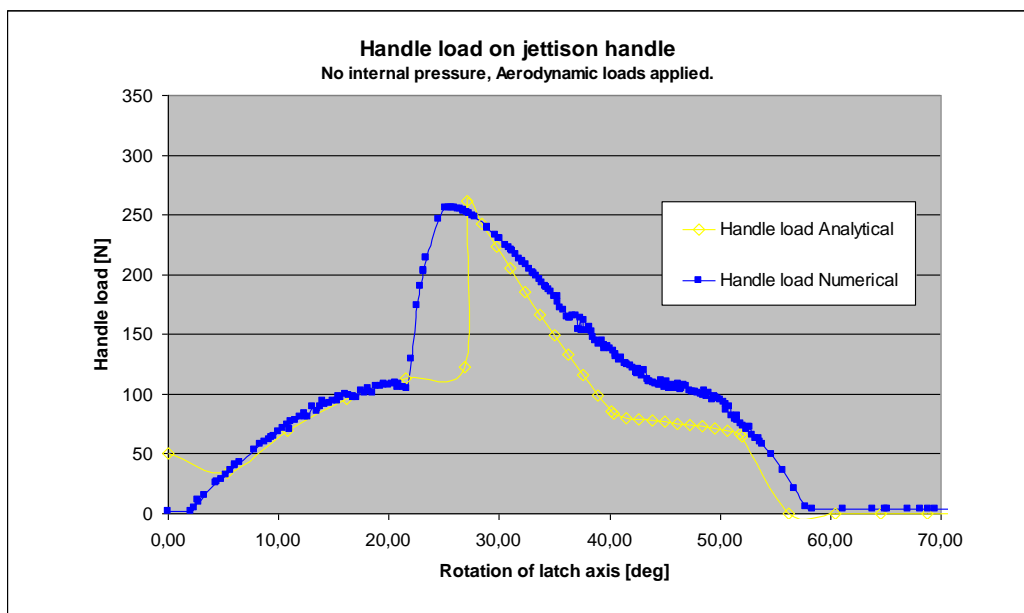
Figure 46. Necessary handle load (limit) on jettison handle to be able to lift the door when subjected to aerodynamic loads but not internal pressure
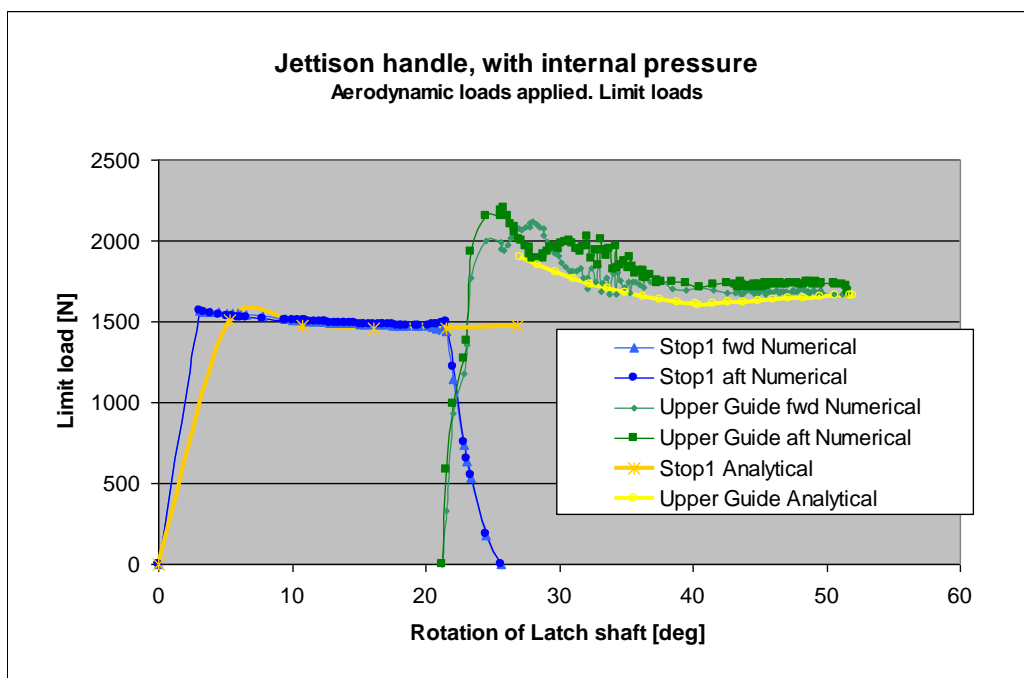
Figure 47. Reaction forces during lifting as a function of latch shaft rotation. Fwd implies forward side hinge and aft implies after side hinge. In the analytical case the forces are assumed to be the same for both sides

	Dokumentslag *Type of document*	Reg-nr *Reg. No*
SAAB	**REPORT-**MSC. Thesis	AIF288-2-RE-0496
	Infoklass *Info. class*	Utgåva *Issue* Sida *Page*
	Öppen	A A-5

Figure 48. Reaction forces during lifting as a function of latch shaft rotation. Fwd implies forward side hinge and aft implies after side hinge. In the analytical case the forces are assumed to be the same for both sides

Jamming during lifting manoeuvre

A jam in the gearbox was created and the forces in rod P7P10 and rod P2P6 were measured when applying a maximal force on the inner, Figure 49, or outer handle, Figure 50, in either opening or closing direction.
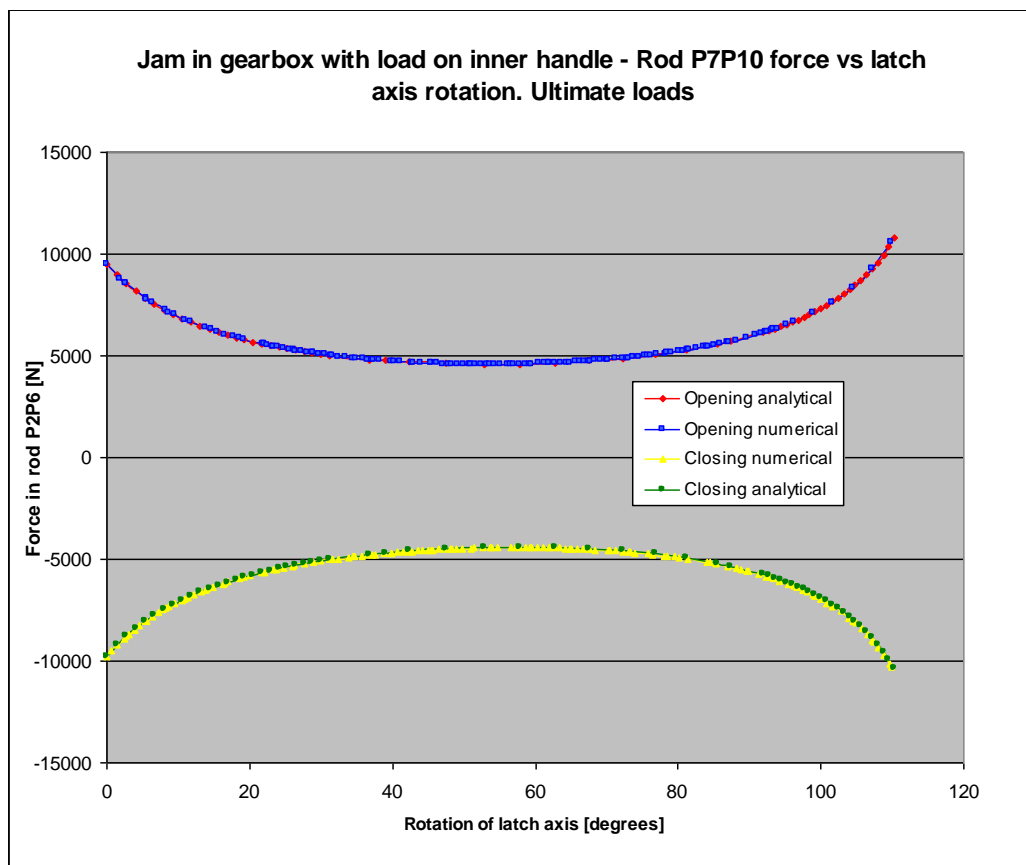
Figure 49. Force in rod P7P10 as a function of rotation of latch axis. Jam in gearbox and an ultimate force (1334N) was applied on the inner handle in either opening or closing direction
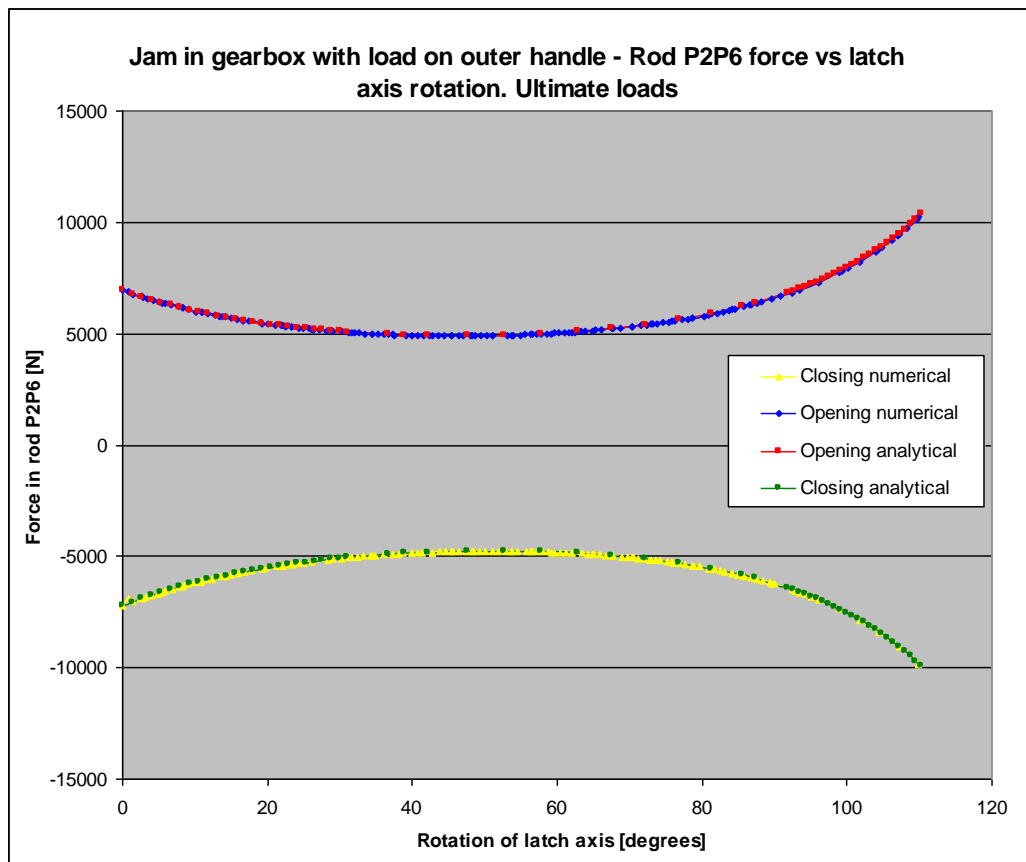
Figure 50. Force in rod P2P6 as a function of rotation of latch axis. Jam in the gearbox and an ultimate force (1334N) was applied on the outer handle in either opening or closing direction

Opening the door

After the door has been lifted it can be opened. The opening movement was controlled by a motion on the CB handle. The motion was programmed to open the door from lifted position in 2.5 seconds. The door was simulated without wind loads, see Figure 51 and Figure 52, and with wind loads in both opening, see report, and closing directions, see Figure 53 and Figure 54.
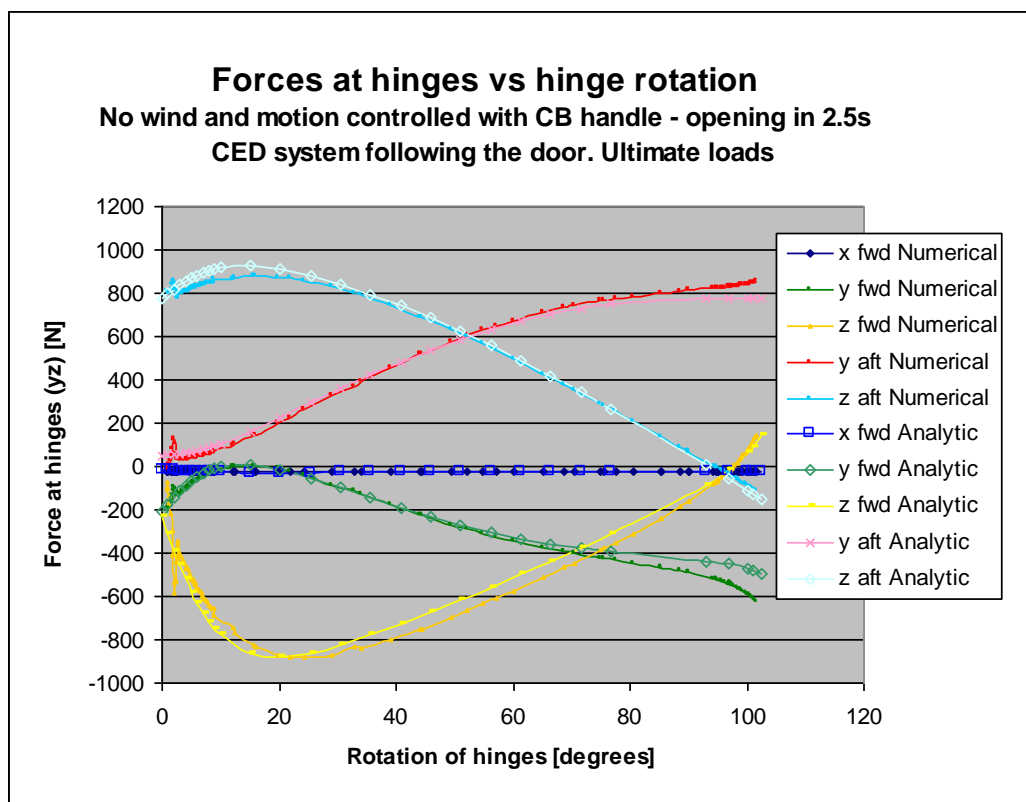
Figure 51. Forces at hinges during opening as a function of opening angle (rotation of hinges). Fwd implies hinge on forward side and aft implies hinge on after side. The movement of the door was controlled by a motion on the CB handle
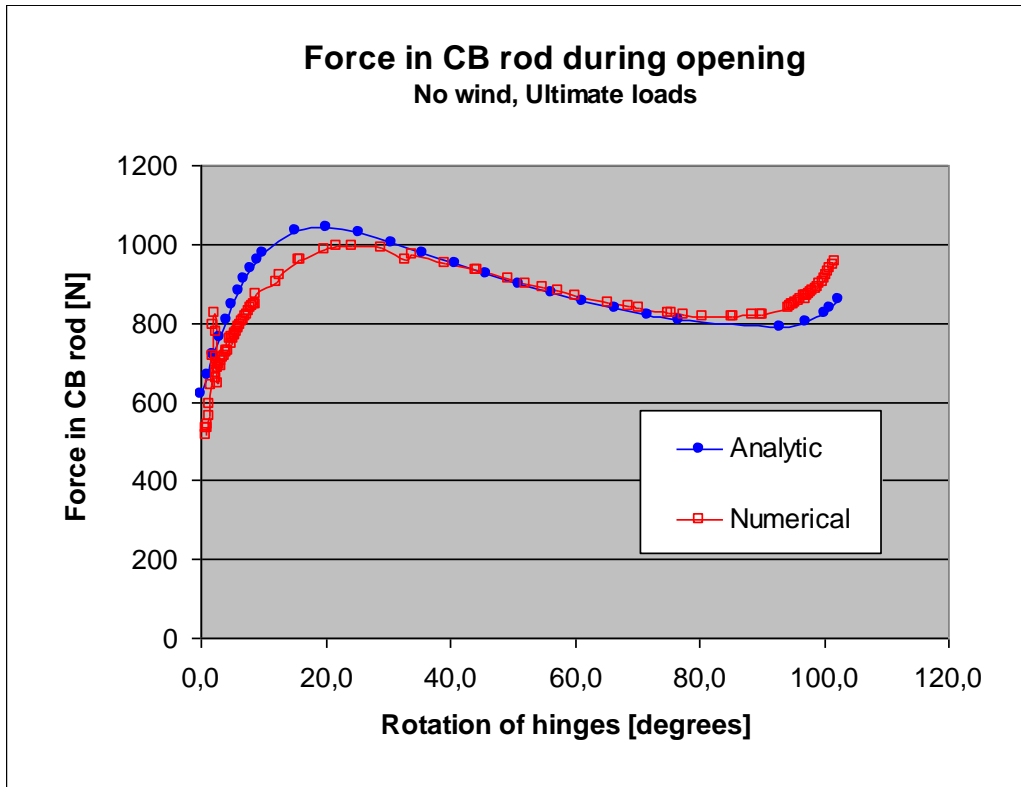
Figure 52. Force in CB rod connection to the door as a function of the opening angle (or rotation of hinges)
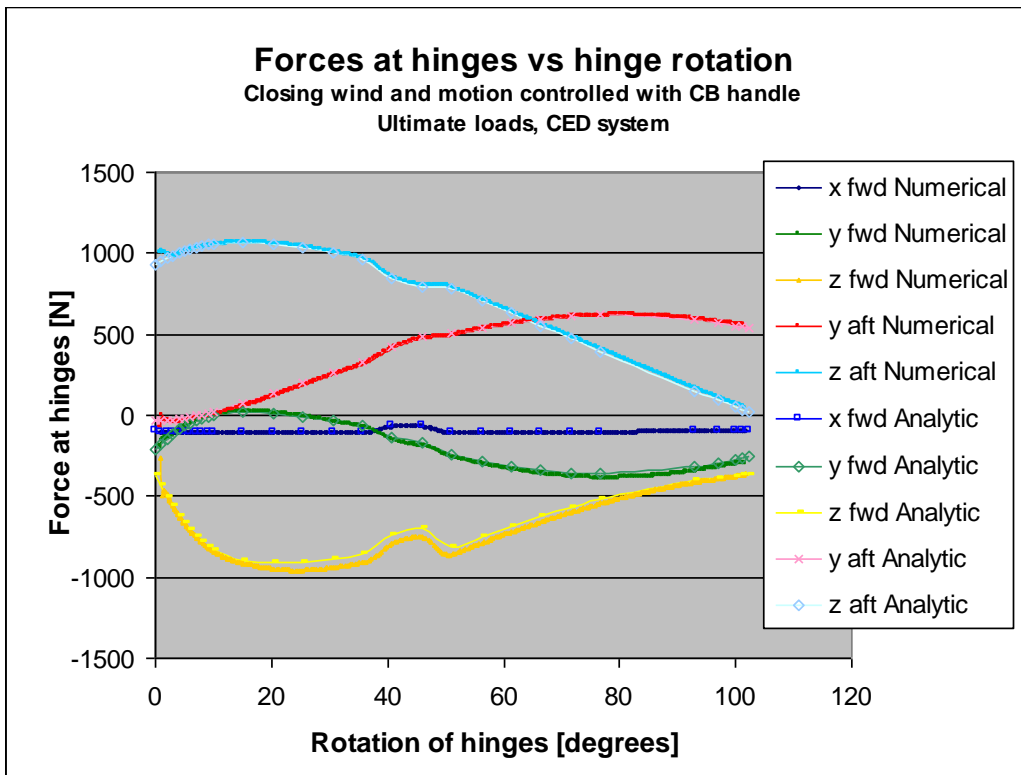
Figure 53. Forces at hinges during opening with wind loads in closing direction applied. Fwd implies hinge on forward side and aft implies hinge on after side. The movement of the door was controlled by a motion on the CB handle
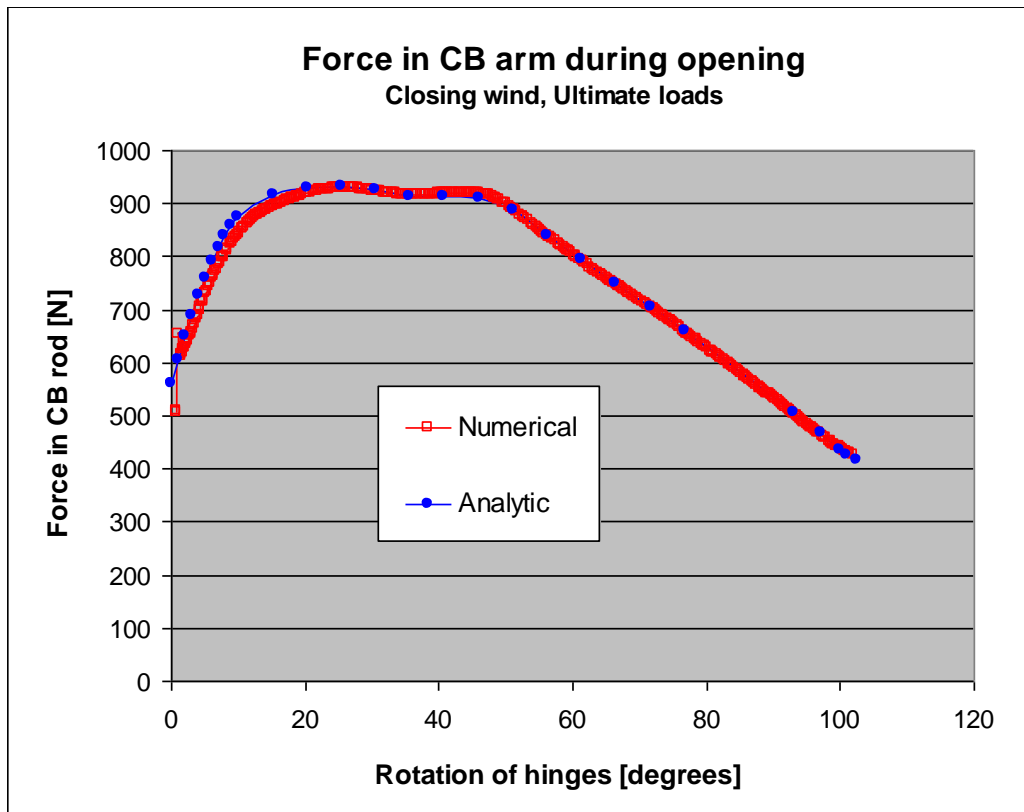
Figure 54. Force in CB rod connection to the door as a function of the opening angle (or rotation of hinges)

Opened door

With the CED in opened position it works as staircase for the crewmembers.

In Figure 55, forces at hinges during some different load cases are presented. For the same cases the forces are also calculated in the CB rod and in the wire and these are presented in Figure 56 and Figure 57 respectively.
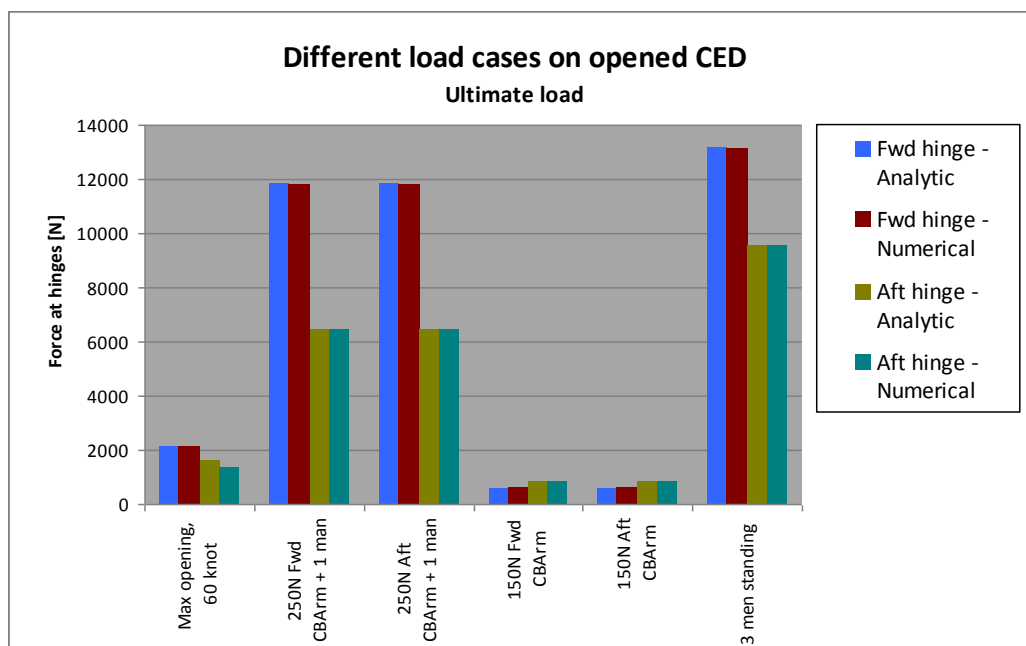

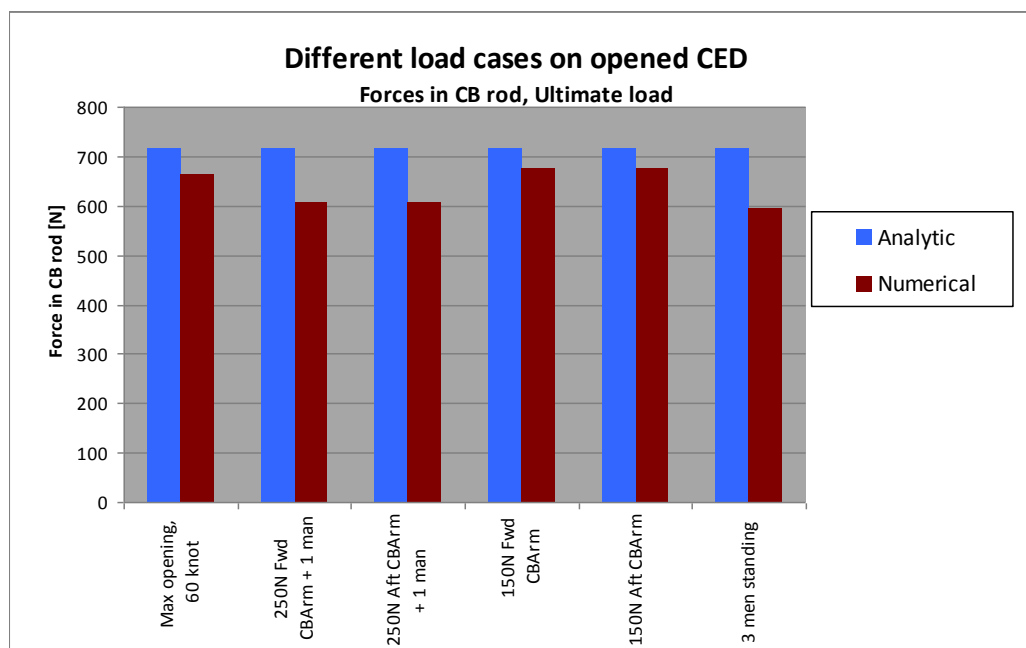Figure 55. Force at hinges for different load cases

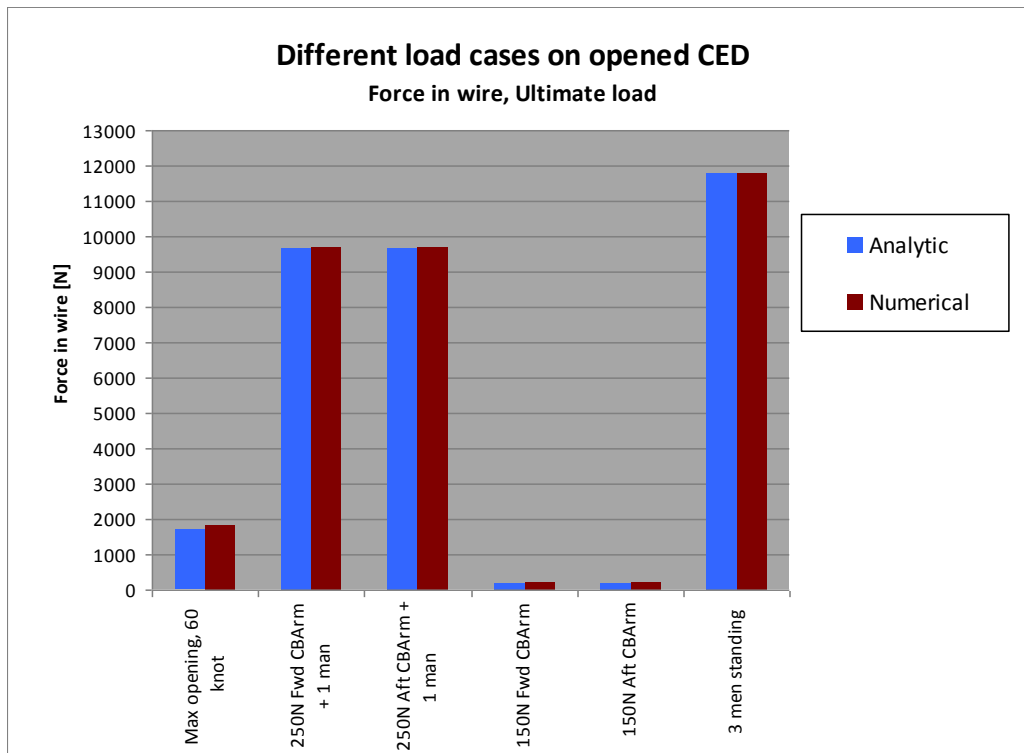Figure 56. Force in CB rod for different load cases

Figure 57. Force in wire for different load cases